Spring 2012

Using Landsat Thematic Mapper Satellite Imagery Assessing And Mapping Trophic State In Cheney Reservoir, Kansas

Dingnan Lu
Fort Hays State University

USING LANDSAT THEMATIC MAPPER SATELLITE IMAGERY ASSESSING AND MAPPING TROPHIC STATE IN CHENEY RESERVOIR, KANSAS

being

A Thesis Presented to the Graduate Faculty

of the Fort Hays State University in

Partial Fulfillment of the Requirements for

the Degree of Master of Science

by

Dingnan Lu

B.S., Fort Hays State University

Date_____ Approved_____
Major Professor

Approved_____
Chair, Graduate Council

ABSTRACT

Eutrophication is a major inland water problem that is researched by many environmentalists and hydrologists. A eutrophic inland water body can cause many negative water problems, such as taste and odor, biotoxin, and low dissolved oxygen. Many previous studies were effective based on using remote sensing to evaluate water body trophic state. In this study, the Cheney Reservoir is selected as an object to test the performance of using remote sensing, specifically the Landsat Thematic Mapper sensor, to evaluate the trophic state of a reservoir. Based on Landsat TM imagery, the chlorophyll a concentration is estimated to be used to indicate the trophic state of the Cheney Reservoir in August, 2011. It is found that the processed Landsat TM images were successfully used to run the regression analysis to assess the whole lake chlorophyll-a concentration, thereby the spatial distribution of trophic state of the Cheney Reservoir in Aug, 2011was done.

During this study, the field measurement and laboratory analysis data were acquired in collaboration with the US Geological Survey in Lawrence, KS. From the results of this study, mean chlorophyll-a concentration is about 10 ug/L, and high-mesotrophic is the dominating trophic state. Both results are comparable with previous studies from Smith in 2001 and 2002. The conclusion of this study is that use remote sensing methods with data of Landsat TM can successfully evaluate the trophic state Cheney Reservoir in August, 2011. The study is limited by the time difference between field measurement and

Landsat TM imagery data, and lack of the same testing on different reservoirs. The major error is from a 14-days difference between the time of image acquisition (August 1, 2011) and the time when the chlorophyll-a measurements were taken (August 15, 2000). In the future work, more attention will put on overcome the mentioned limitation, and reduce error.

ACKNOWLEDGMENTS

This thesis was made possible through the help, advice and support of many individuals. A very special thanks to Dr. John Heinrichs, my advisor, who had the expertise to guide me through many difficult situations. Thanks to the members of my graduate committee, Mr. Bill Heimann, Dr. Paul Adams, and Dr. Richard Lisichenko, for reviewing my thesis and making recommendations along the way. Thanks also to Dr. Jennifer Graham and her team from US Geological Survey Kansas Water Science Center for giving suggestions, arranging the field measurement and analyzing the collected samples.

Also, thanks to my parents, for always being there for me. You will never know how much I appreciate your love and support!

TABLE OF CONTENTS

Page

LIST OF TABLES

LIST OF FIGURES

1. INTRODUCTION

1.1 Importance of Water Resource and Quality

Water is an important resource for all life forms on Earth. Humans rely on water for many different purposes, such as transportation, generation of electricity, cooling, and recreation (Marcello, 2009). Many human uses can reduce water quality, for example, wastewater from coal-burning power plant and dumping of sewage sludge can cause arsenic pollution in a water body (Nriagu & Pacyna, 1988). Low water quality is associated with many significant human health problems, for example, diarrheal diseases, schistosomiasis, trachoma, ascariasis, trichuriasis, and hookworm disease (Pruss, 2002). Disease burden from water, sanitation, and hygiene is 4.0% of all deaths, and also is 5.7% of total disease burden occurring worldwide (Pruss, 2002).

The natural hydrosphere can treat many different types of pollution, because the natural hydrosphere has a powerful capacity for self-purification (Marcello, 2009). However, people sometimes over depend on the capacity of self-purification which is described as a certain type of substance is over the threshold external load of a water body (Nürnberg, 2009). The consequence of exceeding a threshold external load is associated with degradation of water quality and environmental crisis (Nürnberg, 2009). For example, phosphorus from sewage sludge and agriculture in some areas of the Great Lakes exceeds the threshold external load and causes eutrophication in these areas (Nürnberg, 2009).

1.2 Eutrophication and Indicators

1.2.1 Eutrophication

Eutrophication has been defined by different institutions and scientists, and the United State Geological Survey lists four of the prevalent definitions (Committee on Environment and Natural Resources, 2000). Comparing those four definitions, some common points include high concentration of nutrients, excessive growth of algae, depletion of oxygen, and human activity. The most complete definition was proposed by Lawrence and Jackson (1998). The inorganic plant nutrients, nitrate and phosphate enrich the fresh water bodies. The enrichment of fresh water may occur naturally but can also be the result of human activity. For example, cultural eutrophication from fertilizer runoff and sewage discharge is particularly evident in slow-moving rivers and shallow lakes. Increased sediment deposition can eventually raise the level of the lake or river bed, allowing land plants to colonize the edges eventually converting the area to dry land (Lawrence & Jackson, 1998).

Eutrophication processes can be categorized into two different types, natural eutrophication processes and cultural eutrophication processes (Christopherson, 2012). The natural eutrophication process is viewed across geologic time which is considered as a long-term process, so little attention put on natural eutrophication. The definition of natural eutrophication describes a lake or a pond as a temporary feature on the landscape,

because the eutrophication process can gradually fill a lake (Christopherson, 2012). However, humans can accelerate the eutrophication process and cause a eutrophic area of a lake or bond.

Cultural eutrophication usually follows a certain process, and contains four basic processes (Christopherson, 2012). In the beginning stage, the excessive levels of nitrogen and phosphorus, cause from human activities, import into water body. The next stage is the appearance of velvety clumps of blue green algae. When the biomass of blue green algae is over the critical value, the algae possibly will consume the dissolve oxygen to a dangerous level. Eventually all higher life is killed by lack of oxygen (Christopherson, 2012). In some case algae may contain toxins that can also kill of higher life in a short period (Christopherson, 2012).

Another negative impact from water eutrophication is the taste-and-odor problem, which is commonly by-products from algae with no known cellular function (Christensen, Christensen, et al, 2006). Taste-and-odor compounds, became a nationwide concern, can threaten human society by causing unpalatable drinking water, increasing water treatment cost (Christensen, et al, 2006). Geosmin and MIB can cause earthy and musty taste, and are frequently responsible for customer complaints about objectionable drinking water (Christensen, et al, 2006). Taste-and-odor occurrence is also considered as an indicator of the presence of potentially toxic algae (Christensen, et al, 2006). Many taste-and-odor producing cyanobacteria have the potential to produce toxins that may cause illness after exposure through drinking water or recreational activities (Christensen, et al, 2006).

Blue-green algae (cyanobacteria) (Figure 1) and actinomycetes bacteria are two major common bacteria which can produce geosmin and 2-methylisoborneol (MIB). Taste-and-odor occurrence is also considered as an indicator of the presence of potentially toxic algae (Lopez, at all, 2008).

Figure 1 – Cyanobacteria in Binder Lake, Iowa
Source from USGS
http://ks.water.usgs.gov/studies/qw/cyanobacteria/binder-lake-ia.jpg

1.2.2 Indicator – Chlorophyll a

Chlorophyll a is a pigment, essential for photosynthetic process, present in all plants (Jensen, 2000). Chlorophyll a and chlorophyll b are the most important plant pigments absorbing blue and red light: chlorophyll a at wavelengths of 0.43μm and 0.66 μm and chlorophyll-b at wavelengths of 0.45μm and 0.65 μm (Figure 2) (Curran, 1983). Phytoplankton, like plants on land, is composed of substances that contain carbon (Angelo, 2006). All phytoplankton in water bodies contain the photosynthetically active pigment chlorophyll-a, and introducing chlorophyll a into clean water can change the spectral reflectance of water (Jensen, 2000). The spectral reflectance of chlorophyll a is an important parameter for water quality, and usually used for estimation of phytoplankton biomass in a water body (Bee, 2008). Chlorophyll a is one of the many types of chlorophyll and mostly present in algae. High concentration of chlorophyll a in water body indicates a predictable algal bloom event (Longhurst, 1998). Increasing quantity of phytoplankton can result in water pollution and reduction of water dissolved oxygen (Bee, 2008).

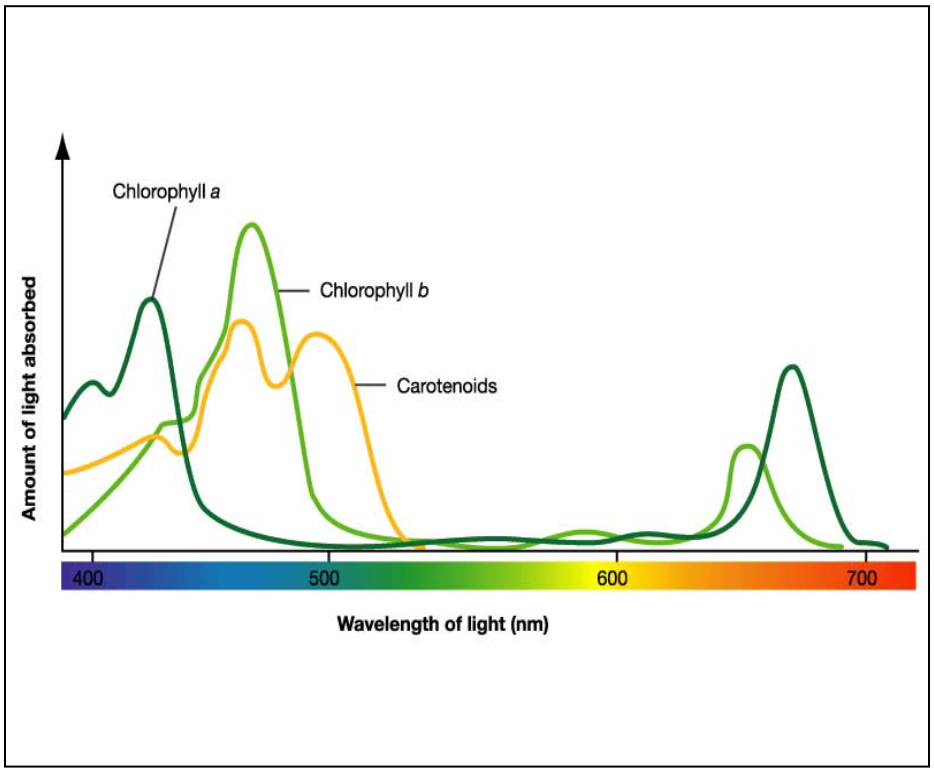

Figure 2 – The Absorbance Spectra of Chlorophyll-a, Chlorophyll-b, and Carotenoids.
Source from University of New Hampshire Center for Freshwater Biology http://cfb.unh.edu/phycokey/Choices/Chlorophyceae/Chl_a_b_carotenoids_absorption-spectrum.jpg

1.3 Using Remote Sensing to Evaluate Water Quality

Pollution sources have two different types, nonpoint source and point source pollution, and the former is more common and more difficult to detect and mitigate (Curran, 1983). In order to trace and evaluate nonpoint source pollution in a large water body, field measurements and sequential laboratory analysis are two important traditional methods (Wang, et al., 2008). However, traditional field measurement or monitoring techniques have some limitations, including high cost, low efficiency, and a lack of real-time characteristic (Wang, et al., 2008). Because the improvements of sensor spatial and spectral resolution, it is possible to use remote sensing information to monitor and assess real-time water quality.

Concentrations of various types of suspended substances related to water quality have been successfully measured based on using remote sensing (Schalles, et al., 1998). The basic principle of using satellite remote sensing to assess an inland water quality is to build a correlation between remote sensing reflectance values and other measured important parameters of water quality, including chlorophyll-a, turbidity, temperature, or Secchi disk depth, which is a conventional measure of the transparency of the water (Bledzki, 2009). Compared with traditional sampling technique, remote sensing can effectively reflect the real-time spatial distribution of water pollution and changing of water quality, and is able to separate the concentration distribution and locate the pollution source (Curran, 1983).

1.4 Landsat TM Imagery and Previous work with Landsat TM Data

1.4.1 Introduction of Landsat TM Sensor

Landsat Thematic Mapper sensor systems were launched on July 16, 1982 (Landsat 4), and on March 1, 1984 (Landsat 5) (Jensen, 2000). The TM is a scanning optical-mechanical sensor that records energy in the visible, near-infrared, middle-infrared, and thermal-infrared regions of the electromagnetic spectrum (Jensen, 2000). The Landsat Thematic Mapper (TM) collects a multispectral imagery that has higher spatial, spectral, temporal, and radiometric resolution. The Landsat TM sensor system's characteristics are shown in Table 1. For remote sensing study, the Landsat TM bands can make maximum use of the dominant factors controlling leaf reflectance (Jensen, 2000), and this characteristic is rather important for detecting chlorophyll-a in a water body.

Table 1 – Landsat Thematic Mapper Bands Distribution and Wavelength. (Jensen, 2000)

TM Band	Wavelength (μm)	Resolution (m)	Band Name
7	10.4 – 12.5	30 *30	Thermal Infrared
6	2.08 – 2.35	120 *120	Shortwave Infrared
5	1.55 – 1.75	30 *30	Shortwave Infrared
4	0.76 – 0.90	30 *30	Near Infrared
3	0.63 – 0.69	30 *30	Red
2	0.52 – 0.60	30 *30	Green
1	0.45 – 0.52	30 *30	Blue

1.4.2 Previous Studies on Remote Sensing of Chlorophyll-a Using Landsat Imagery (Miyun, Reservoir, Beijing, China)

There have been some successful projects in China, the U.S., and Europe in using Landsat Thematic Mapper imagery to evaluate the eutrophic state in lakes, reservoirs, even coast zone. One successful project was performed on Miyun Reservoir, Beijing, China which used data from Landsat TM (Wang, Hong, & Du, 2008). Two Thematic Mapper images in May and October of 2003 were acquired and simultaneous in situ measurements, sampling and analysis were conducted (Wang, Hong, & Du, 2008). Three satellite-based normalized ratio vegetation indexes were involved in the analysis, including normalized difference vegetation index (NDVI), ratio vegetation index (RVI), and normalized ratio vegetation index (NRVI). The result from linear regression models and determination coefficients show NRVI had great correlation coefficient of 0.95 with measured water chlorophyll-a concentration. The final product of this research about Miyun Reservoir was a trophic state index map (Figure 3), showing the spatial distribution of trophic situation of Miyun Reservoir in two distinctive seasons. This trophic state index map is a fine example of remote sensing studies.

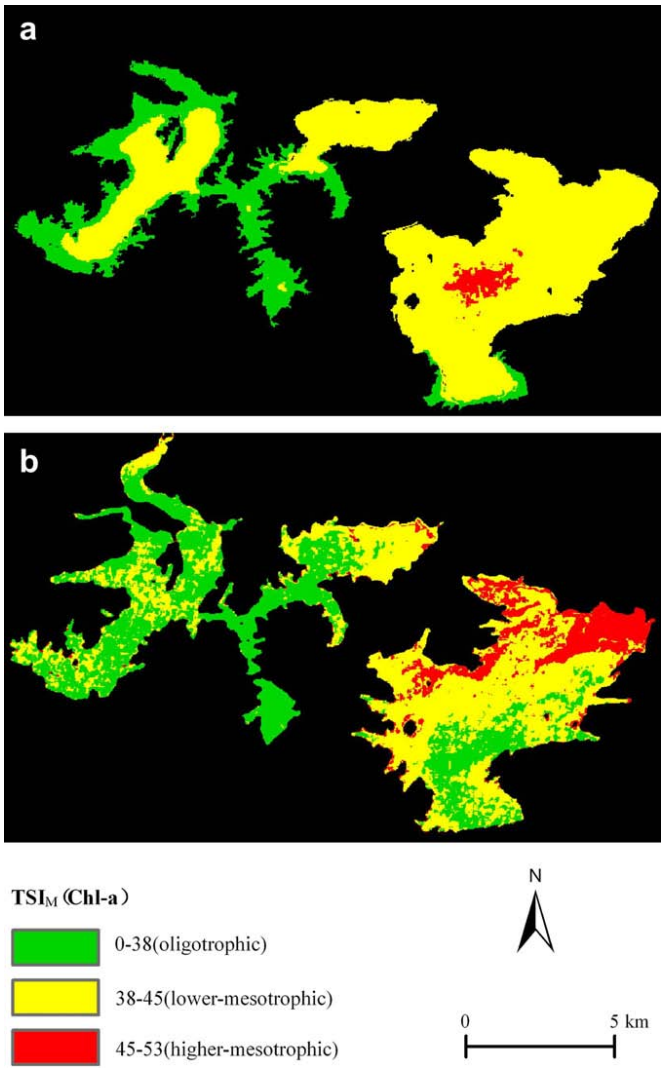

Figure 3 – Trophic State Distribution Map of Miyun reservoir in May and October in 2003 (Wang, et al., 2008).

1.4.3 Previous Studies on Remote Sensing of Chlorophyll-a Using Landsat Imagery (Ohio River, U. S.)

In a study done by Shazia Bee (2008), the focus was on a 95 km segment of the Ohio River, where the USEPA had collected turbidity and chlorophyll a samples the same day as the Landsat 7 overpass. The statistics methods involved the Pearson correlation coefficient and a linear regression model, and all indicated a high correlation between chlorophyll a and turbidity indices (figure 4, figure 5). The annual and seasonal variation of turbidity was analyzed based on building the correlation between the USEPA collected turbidity and satellite-based turbidity reflectance. The result from analysis of annual variation of turbidity showed a significant decrease in the concentration of turbidity from the year 2002, indicating improvement in the water quality (Bee, 2008).

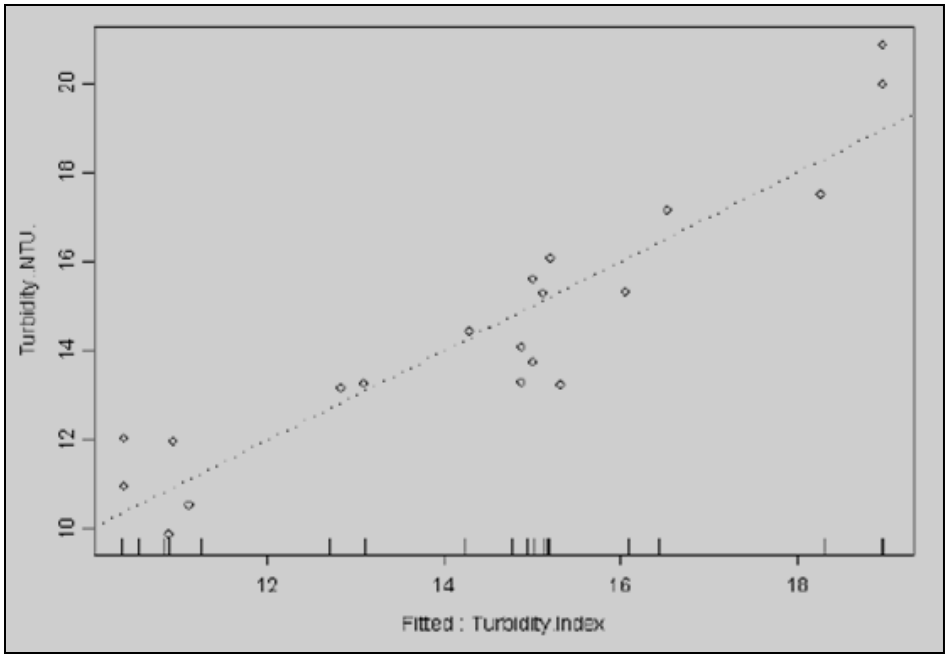

Figure 4 – Linear Regression Plot of Actual Turbidity (NTU) vs. the Turbidity Index. (Frohn, & Autrey, 2009)

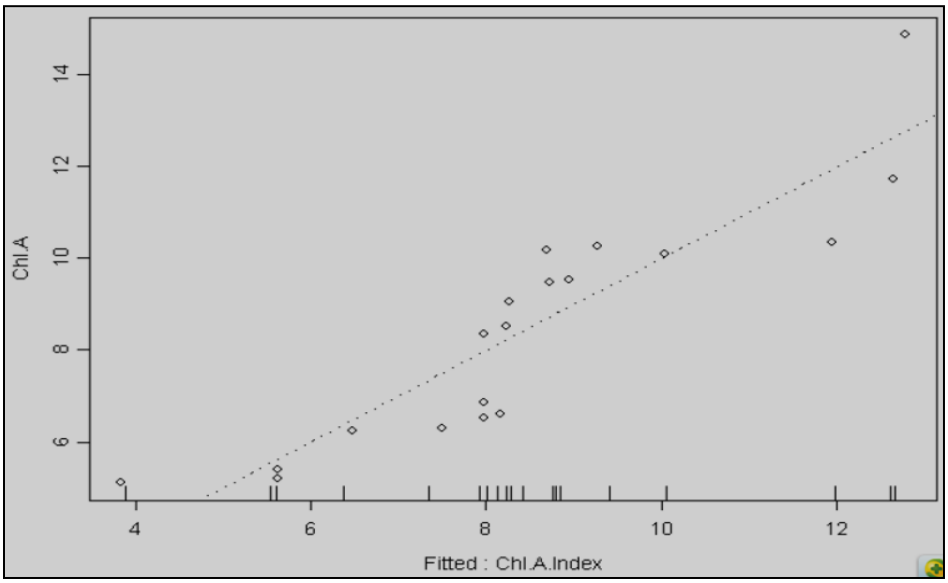

Figure 5 – Linear Regression Plot of Actual Chlorophyll-a vs. the Chlorophyll-a Index.
(Frohn, & Autrey, 2009)

1.5 Problem Statements and Project Objectives

Due to the importance of water resource and quality, and the difficulties of using traditional measurement to monitor nonpoint source pollution and eutrophic situation of a water body, developing a new approach to evaluate trophic state becomes highly necessary. The objective of this study is to test the method of using Landsat TM imagery data to assess and map the real-time spatial distribution of trophic state of a water body, specifically the Cheney Reservoir in Kansas.

2. METHODS

In this research the basic principle of the method is to explore the statistical relations between satellite-based data and field measurements and lab analysis data, and meanwhile using different mathematical models to express these relations, and then applying geographic information system (GIS) software – ArcMap to map the trophic statement of the Cheney Reservoir in August, 2011.

2.1 Study Area

In order to test the performance of Landsat TM imagery data for evaluating a reservoir's trophic state, Cheney Reservoir selected as a pilot object in this study mainly due to its historical frequent occurrences of eutrophication events and taste-and-odor problems.

Cheney Reservoir (figure 6) was constructed by the Bureau of Reclamation (BOR), U.S. Department of the Interior, between 1962 and 1965 to provide downstream flood control, wildlife habitat, recreational opportunities, and a reliable municipal water supply for the city of Wichita, Kansas, roughly 70 % of the daily water supply for the city of Wichita, providing about 350,000 residents in the Wichita area (Christensen, et al., 2006).

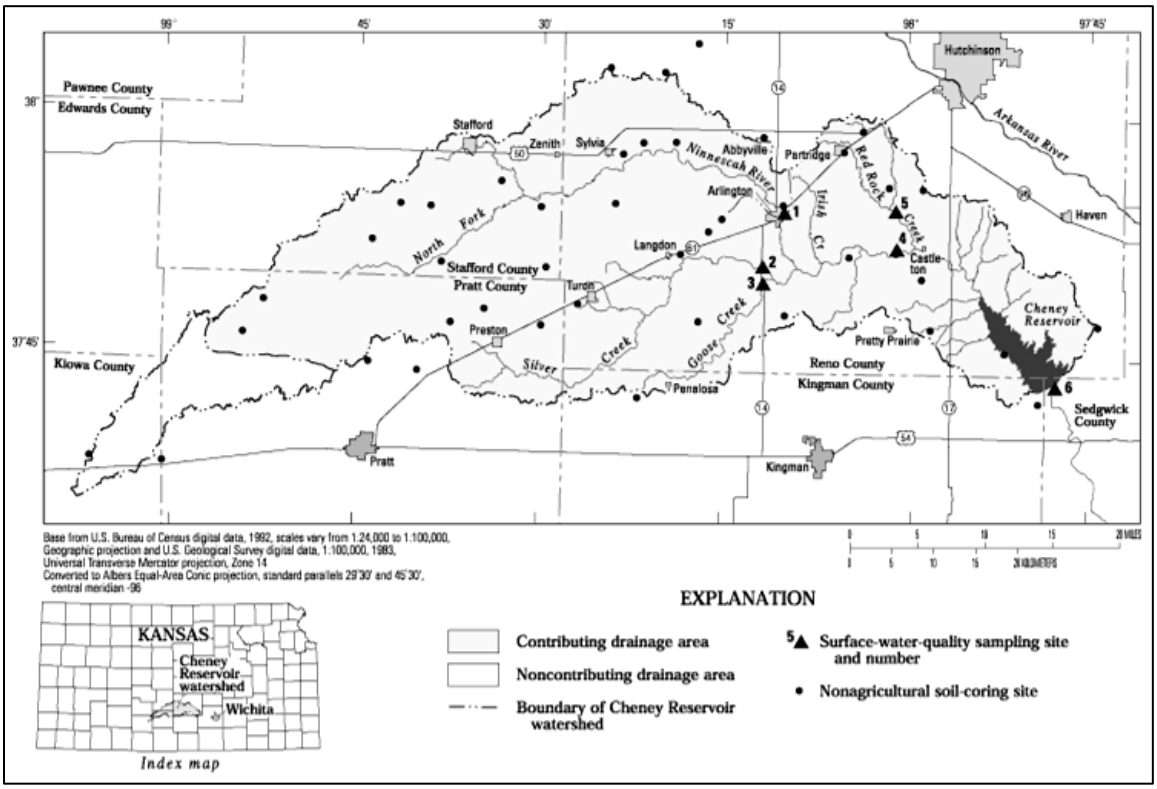

Figure 6 – Location of Cheney Reservoir and Its Watershed.
Source from USGS

The treatments of solving taste-and-odor problems are costly and seldom succeed completely (Wang, et al., 2008). Many actions, including study contamination problem, develop water quality goals, and implement programs, were launched by different individuals and organizations for response to the 1990-91 taste-and-odor occurrences in Cheney Reservoir (Christensen, et al., 2006). In order to monitor algal growth and taste-and-odor problems, a monitoring program implemented in Cheney Reservoir watershed by the U.S. Geological Survey (USGS), in cooperation with the city of Wichita. This program monitored phosphorus and other suspended-solids concentrations and yields in the North Fork Ninnescah River above Cheney Reservoir from 1997 to 2008.

Another water quality program implemented for Cheney Reservoir, named best-management practices (BMPs), limits the flow of physical, chemical, and biological water-quality constituents into the reservoir (Christensen, et al., 2006). BMPs in the Cheney Reservoir watershed include but are not limited to field terracing, stubble mulch, grassed waterways, and efficient fertilizer application (Christensen, et al., 2006).

2.2 Refining of Water Body

A watershed is a region (or area) delineated with a well-defined topographic boundary and water outlet, and is a geographic region within which hydrological conditions are such that water becomes concentrated within a particular location, for example, ocean, sea, lake, river, or reservoir, by which the watershed is drained (Nath & Deb, 2010).

In many cases, refining a water body to separate from a satellite image is a crucial preliminary step for remote sensing studies. Within the topographic boundary or a water divide, watershed comprises a complex of soils, landforms, vegetations, and land uses (Nath & Deb, 2010). So, a common challenge occurring during water body extraction is how to acquire outline of a water body or catchment accurately. From Nath and Deb's work (2010), three major types of water extraction were introduced, including extracted features methods, supervised classification methods, and unsupervised classification methods. The classification method used in this research is maximum likelihood classification, which belongs to the supervised classification methods. In maximum likelihood classification, the process of selecting the "Region of Interest" provides the criteria for classification, and in this case two types of regions involved, which are land and water. The last step is to implement the maximum likelihood classification function based on the selected pixel samples.

2.4 Selecting the Algorithms

A good algorithm can filter the useful information for a remote sensing analysis, and whether an algorithm is good depends on the differences of natural characteristics of reflectance between non-algae water and algae-laden water. Figure 7 depicts the spectral reflectance characteristics of clear water and the water laden with algae consisting primarily of chlorophyll-a (Han, 1997).

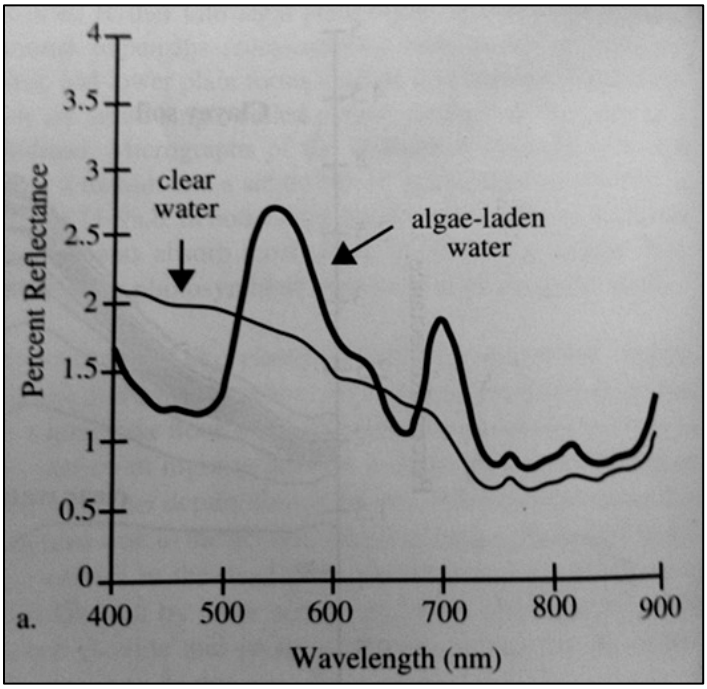

Figure 7 – Percent Reflectance of Clear and Algae-laden Water Based on In Situ Spectroradiometer Measurement (Han, 1997).

From the above figure, the biggest difference roughly locates at the wavelength during 500 nm to 700 nm, so the proposed algorithms for this study mainly focus into this range of wavelength. In order to find the useful band(s) associated with algae-laden water, Landsat TM bands are added on Figure 7 to produce Figure 8.

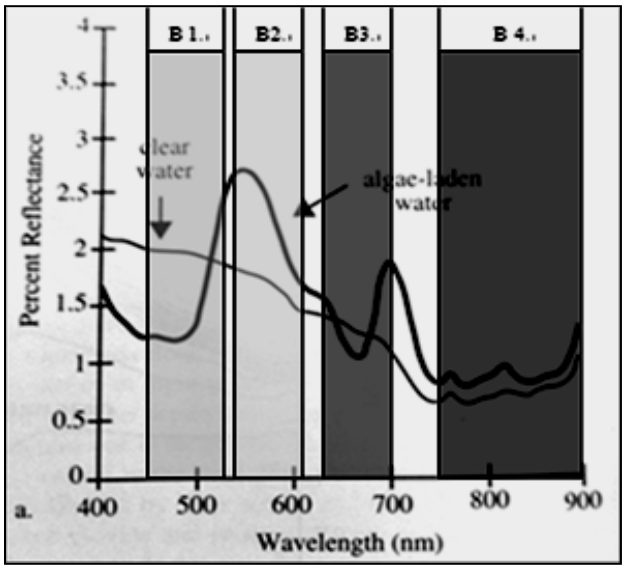

Figure 8 –Percent Reflectance of Clear and Algae-laden Water Based on In Situ Spectroradiometer Measurement with Four Band Ranges of Landsat TM (adapted from Han, 1997).

From Figure 8, the band 1 and band 3 all are located at the absorption peaks of algae; band 2 are located at the reflectance peak of algae. Band 4 shows that algae have no effect on water reflectance in this range. Knowing characteristics of band 2, 3, and 4 is not enough to determine an optimal algorithm.

Exploration of the reflectance characteristics changing during different water quality is a logical second step for finalizing the focusing bands. When the concentrations of suspended solids change, band 1 and band 2 are not sensitive. However band 3 shows significant differences between non-algae water and algae-laden water. Moreover, band 4 has no responses to the presence of algae, so can be considered as a reference value in an algorithm.

With all the above detailed information, three different algorithms were pre-selected for further analysis:

1. Reflectance = Band 3
2. Reflectance = Band 4 / Band 3 (Simple Ratio)
3. Reflectance = (Band 3 – Band 4) / (Band 3 + Band 4) (modified Normalized Difference Vegetation Index)

2.5 Imagery Parameters

One Landsat TM image is selected for this study. The image was acquired on August 1, 2011 through Landsat 5 TM sensor, and based on World Reference System the image was on the path 28, and row 34.

A black and white image is provided to show the coverage of one particular satellite image (figure 9); Cheney Reservoir and City of Wichita are highlighted by black boxes. Another image (figure 10) provides a general contour of Cheney Reservoir from Landsat TM image.

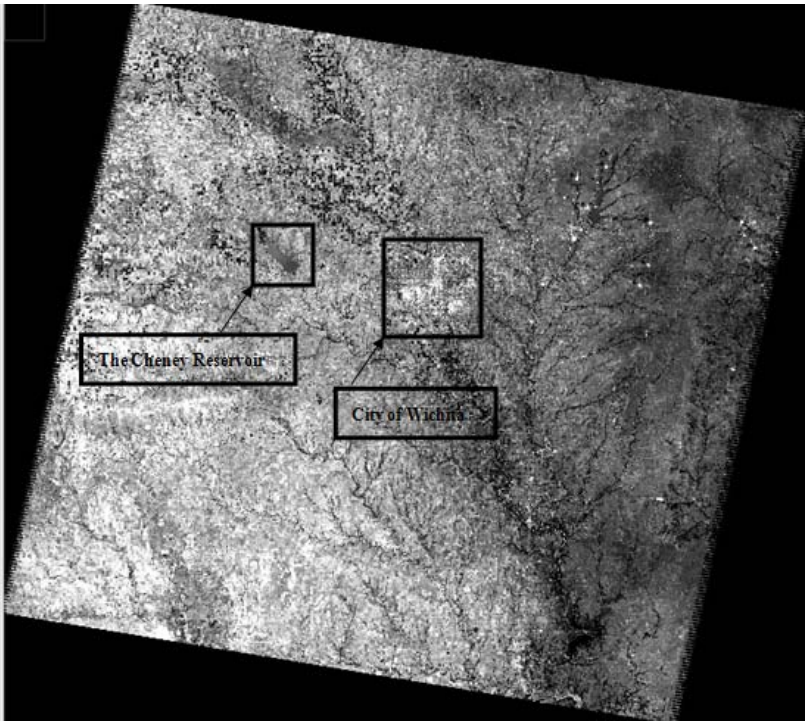

Figure 9 – Landsat TM Imagery on August 1, 2011 at Path 28 – Row 34

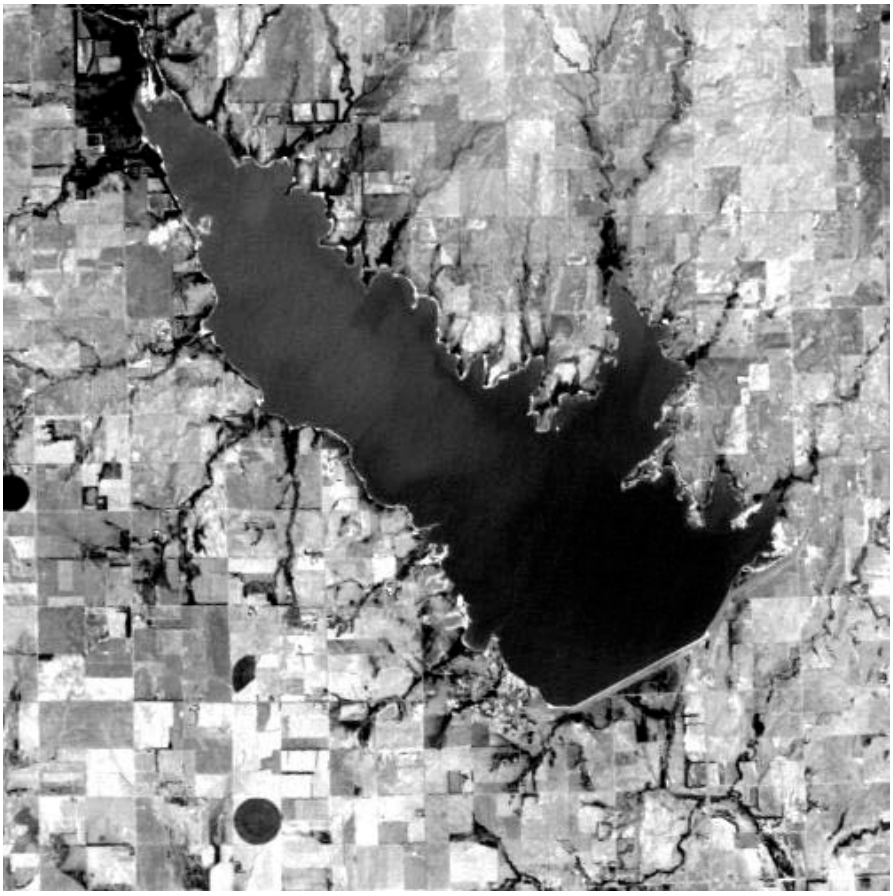

Figure 10 – Cheney Reservoir on Landsat TM Imagery (Band 2 only).

2.6 Field Measurement and Lab Analysis

Carried out in collaboration with the USGS Office in Lawrence, KS, and the USGS Field Lab in Wichita, KS, this research is able to collect data from Cheney Reservoir. A total number of 45 sample sites were acquired in August 15, 2011, and the sample pattern shows in the figure 8, and the sampling sites location information lists in table 1.

In this study, the west part of Cheney Reservoir, high historical chlorophyll a concentration area, is designed as the focus area than the east. The sampling pattern was drawn to bring out a disproportional stratified sampling pattern. The way of disproportional stratified sampling pattern was well described in McGrew and Monroe's work (2009). The major purpose of disproportional stratified sampling pattern is to oversample the focused zone to have more samples of west. A nearest neighbor analysis is used to check if the sampling patter is more clustered. The processes and formulas for nearest neighbor analysis are provided as below:

$$\overline{\mathrm{NND_R}} = \frac{1}{2 * \sqrt{\mathrm{Density}}}$$

Where $\overline{\mathrm{NND_R}}$ = average nearest neighbor distance in a random pattern

Density = number of points (n)/area

$$\mathrm{R} = \frac{\overline{\mathrm{NND}}}{\overline{\mathrm{NND_R}}}$$

Where $\overline{\mathrm{NND}}$ = average nearest neighbor distance

$$\mathrm{Z_n} = \frac{\overline{\mathrm{NND}} - \overline{\mathrm{NND_R}}}{\sigma_{\overline{\mathrm{NND}}}}$$

Where $\sigma_{\overline{NND}}$ = standard error of the mean nearest neighbor distances

The sampling activity is based on the samples map (Figure 11) to collect each sample. The major instruments used on the sampling activity are included, GPS, YSI 6600 EDS sonde (figure 12 left), and Secchi disk (figure 12 right). The GPS provides accurate location information for each sample site (Table 2). Data collected include specific conductance, pH, water temperature, turbidity, dissolved oxygen, blue-green algae, and chlorophyll. The sonde was calibrated in accordance with standard USGS procedures (Wagner, 2006). Secchi depth was measured using a standard 200 mm disk. In order to obtain more accurate chlorophyll-a data, for each site, the water sample was sent to USGS Kansas Water Science Center for fluorometric analysis.

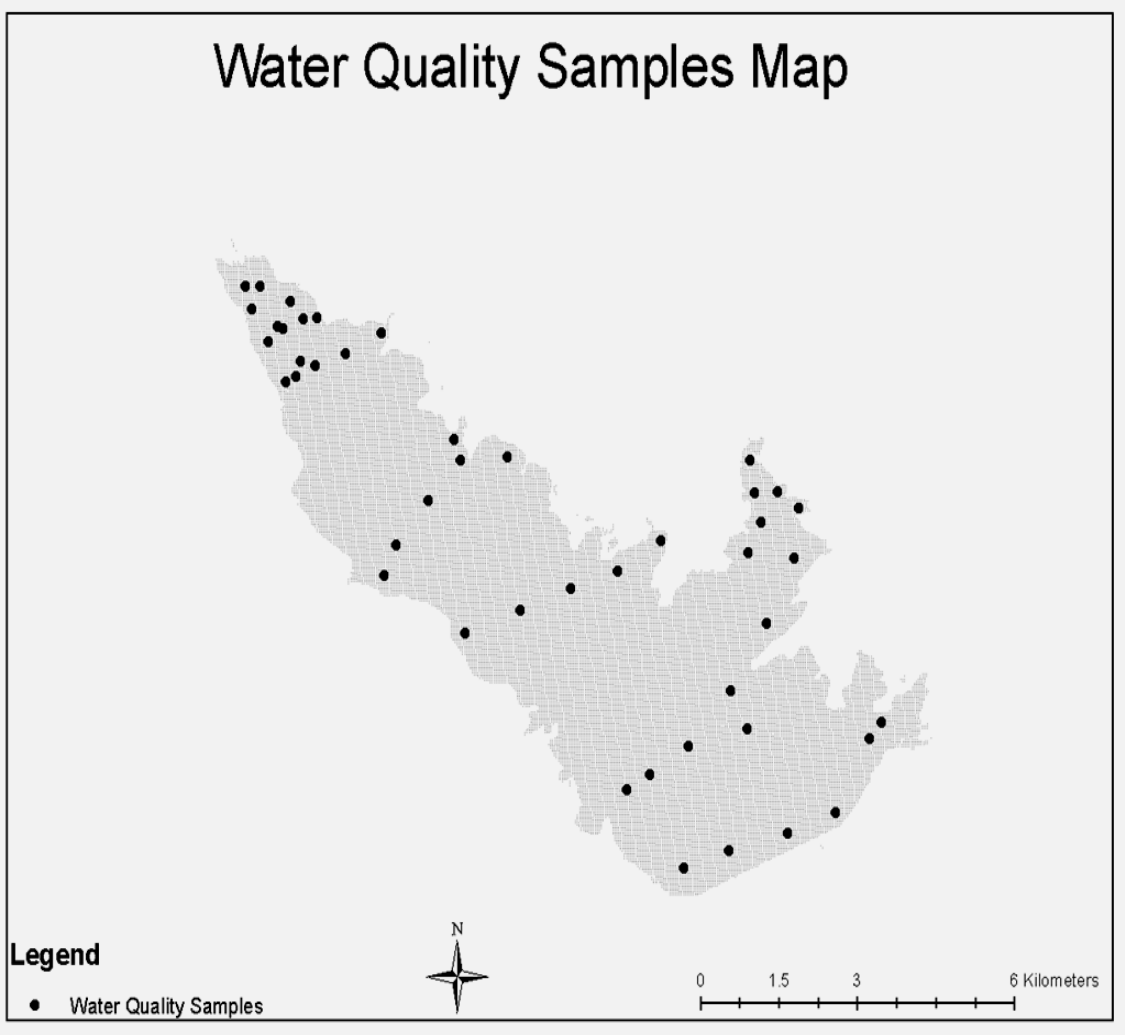

Figure 11 – In Situ Water Sampling Sites Map on 15 Aug, 2011 at Cheney Reservoir.

Figure 12 –Image of YSI 6600 EDS Sonde (left), and Image of Secchi Disk (right).

Table 2-- Sample Site Location					
Sample ID	Latitude	Longitude	Sample ID	Latitude	Longitude
1	37°44'34" N	97°47'01"W	24	37°45'21" N	97°51'18"W
2	37°44'26" N	97°47'08"W	25	37°45'51" N	97°52'08"W
3	37°43'47" N	97°47'29"W	26	37°46'07" N	97°52'01"W
4	37°43'36"N	97°47'59"W	27	37°46'30" N	97°51'41"W
5	37°43'27"N	97°48'35"W	28	37°46'51" N	97°51'21"W
6	37°43'18"N	97°49'63"W	29	37°47'02" N	97°51'25"W
7	37°43'59"N	97°49'38"W	30	37°46'53" N	97°50'52"W
8	37°44'07"N	97°49'24"W	31	37°47'58" N	97°52'10"W
9	37°44'22"N	97°49'00"W	32	37°47'47" N	97°52'32"W
10	37°44'31"N	97°48'24"W	33	37°47'41" N	97°52'51"W
11	37°44'51"N	97°48'34"W	34	37°47'35" N	97°53'03"W
12	37°45'26"N	97°48'12"W	35	37°47'32" N	97°53'09"W
13	37°46'00"N	97°47'55"W	36	37°47'53" N	97°53'20"W
14	37°46'26"N	97°47'52"W	37	37°47'60" N	97°53'11"W
15	37°46'35"N	97°48'05"W	38	37°48'05" N	97°52'58"W
16	37°46'51"N	97°48'22"W	39	37°48'06" N	97°52'50"W
17	37°46'34"N	97°48'19"W	40	37°48'14" N	97°53'06"W
18	37°46'19"N	97°48'15"W	41	37°48'22" N	97°53'25"W
19	37°46'03"N	97°48'23"W	42	37°48'22" N	97°53'34"W
20	37°46'09"N	97°49'17"W	43	37°48'10" N	97°53'30"W
21	37°45'53"N	97°49'44"W	44	37°48'01" N	97°53'14"W
22	37°45'44"N	97°50'13"W	45	37°47'43" N	97°52'00"W
23	37°45'33"N	97°50'44"W			

2.7 Pearson's Correlation Coefficient Analysis

The most powerful and widely used index to measure the association or correlation between two variables is Pearson's product-moment correlation coefficient (McGrew & Monroe, 1993). The primary function of Pearson's correlation analysis is to determine if an association exits between two groups of variables. The principle of Pearson's correlation coefficient is close to covariation, it depicts the degree of two groups of variables' relation (McGrew & Monroe, 1993). If the values of the two variables covary in a similar manner, the variables contain a large covariation, so they have strong correlation (McGrew & Monroe, 1993).

In this study, processed image pixel values and in situ data are pairs of variables, and correlation coefficient analysis implement between them. Image pixel values are processed based on the three distinctive algorithms. In situ data include field measurement and laboratory analysis. Since the correlation coefficient analysis can only test the relationship between two variables, three different algorithms processed results and two groups of in situ data add together to build six different correlations. Six correlation coefficients are generated from this analysis with different values, and each of them represents a possible correlation coefficient between satellite-based data and in situ data. The analyses of Pearson's correlation coefficient in this study were all performed by using Microsoft Excel 2007.

Another reason for choosing Pearson's correlation coefficient is because the analysis

results can be evaluated the significance on a specific confidence level based on t-test analysis. In this analysis of correlation, the rejected null hypothesis is that no significant correlation coefficient exists between the satellite-based data and in situ data. The alternative hypothesis is that either a strong negative or positive correlation coefficient exists between them.

2.8 Regression Analysis

In correlation coefficient analysis, a functional or causal relationship between the two variables is not available. However, a regression analysis is a useful statistical procedure that supplements correlation (McGrew & Monroe, 1993). Since the former correlation coefficient analysis has six possible results, logically the regression analysis as the supplementary process, also implement six times respectively. In the process of regression analysis, because satellite-based data is used to evaluate the estimated chlorophyll-a concentration, the pixel values processed based on different algorithms is the independent variable “x”, and the estimated chlorophyll-a concentration is the dependent variable “y”. A coefficient of determination is calculated to determine the variation in the concentration data explained by the processed pixel values.

In the most common application of regression analysis is the identification of linear relationships between two variables (McGrew & Monroe, 1993). In the situation of linear form, changes in the variables are constant across the range of data.

The regression analysis is implemented using the function of Data Analysis from Microsoft Excel 2007. The typical results from regression analysis is included an equation, a percentage coefficient of determination, and a regression diagram.

2.9 Trophic State Index Analysis

The trophic status refers to the level of productivity in a lake as measured by phosphorous, algae abundance and depth of light penetration (Sharma, Kumar, & Rajvanshi, 2010). Trophic State Index (TSI) is used to rate an individual water body with its amount of biological productivity. Using the index, one can get a quick idea about the extent of productivity of a lake (Hillsborough, 2008). TSI values can be used to indicate the spatial pattern among regions. This ranking enables the water managers to target lakes that may require restoration or conservation activities. An increasing trend in TSI over a period of several years may indicate the degradation of the health of a lake. Table 3 reviews the different types of TSI developed and the corresponding main lake characteristics (Sharma, et al., 2010).

In this study, Carlson's Trophic States Index is used to determine TSI. The Carlson's equations (Sharma, Kumar, & Rajvanshi, 2010) involve three distinct parameters, which are total phosphorous, chlorophyll-a concentration, and Secchi depth. Due to the primary focusing on chlorophyll-a concentration, chlorophyll-a concentration is the only parameters. The modification was also used once in by Christensen, Graham, Milligan, Pope and Ziegler (2006)'s work. The modified Carlson's Trophic State Index Equation is:

TSI = 30.6 + 9.81 Ln [Chlor-a] (ug/L); Where chlor 'a' is chlorophyll-a.

In figure 18, Carlson's Trophic State Index is ranked by the assigned value of TSI.

TSI	Status	Status of lakes
< 30	Oligotrophy	Classical Oligotrophy: Clear water, oxygen throughout the year in the hypolimnion, salmonid fisheries in deep lakes.
30-40	Mesotrophy	Deeper lakes still exhibit classical oligotrophy, but some shallower lakes become anoxic in the hypolimnion during the summer.
40-50	Mesotrophy	Water moderately clear, but increasing probability of anoxia in hypolimnion during summer
50-60	Eutrophy	Lower boundary of classical eutrophy: Decreased transparency, anoxic hypolimnia during the summer, macrophyte problems evident, warm-water fisheries only.
60-70	Eutrophy	Dominance of blue-green algae, algal scums probable, extensive macrophyte problems.
70-80	Hyper eutrophy	Heavy algal blooms possible throughout the summer, dense macrophyte beds, but limited light penetration.(Often would be classified as hypereutrophic)
> 80	Hyper eutrophy	Algal scums, summer fish kills, few macrophytes, dominance of rough fish etc.

Table 3 – Carlson's Trophic State Index (Sharma, et al., 2010).

3. Statistical and Analysis Results

Table 4 through 6 shows the results of field measurement, lab fluorometric analysis, and the Landsat TM image pixel values of all the 45 samples. Table 7 lists the six pairs of correlation coefficients between satellite-based values and in situ data. The graphical results of each regression are shown in figure 13 through 18. Estimated chlorophyll a concentration maps are shown in Figure 16 through 22, and the final trophic state maps are shown in Figure 23 through 29.

Table 4 Field Measurement Data and Lab Analysis Data from Each Sampling Site, and the Imagery Pixel Value of Spatial Corresponding Location. (Imagery processed by Algorithm 1)

Sample ID	Field (ug/L)	Lab (ug/L)	Pixel Value	Sample ID	Field (ug/L)	Lab (ug/L)	Pixel Value
1	5.3	3.21	0.557	24	5.7	12.04	0.495
2	5.2	2.37	0.531	25	6.6	5.96	0.516
3	3.9	2.93	0.554	26	8.7	18.04	0.472
4	4.2	1.22	0.572	27	6	9.08	0.490
5	4.5	2.89	0.545	28	7.3	10.91	0.495
6	4.8	2.05	0.545	29	5.5	3.24	0.500
7	5.5	2.66	0.552	30	7.7	11.48	0.495
8	5	3.9	0.546	31	9.8	10.86	0.495
9	4.4	3.18	0.517	32	9.3	9.66	0.490
10	5.2	3.51	0.556	33	12.7	12.07	0.475
11	5.1	4.86	0.571	34	8.8	9.26	0.488
12	5.4	8.21	0.516	35	8.2	10.06	0.488
13	5.9	7.37	0.516	36	9.6	14.23	0.472
14	6.4	4.9	0.545	37	16.08	19.71	0.462
15	5.8	15.41	0.500	38	17.06	17.52	0.475
16	10.6	6.79	0.523	39	10.6	9.77	0.476
17	8.1	8.47	0.516	40	11.4	6.25	0.487
18	6.4	12.98	0.495	41	13.9	7.48	0.488
19	6.1	11	0.501	42	10.6	10.88	0.472
20	8.3	9.46	0.510	43	12.7	11.32	0.475
21	3.9	4.84	0.546	44	18.7	35.45	0.462
22	5	4.17	0.542	45	7.5	10.49	0.475
23	6.3	8.69	0.512				

Table 5– Field Measurement Data and Lab Analysis Data from Each Sampling Site, and the Imagery Pixel Value of Spatial Corresponding Location. (Imagery processed by Algorithm 2)

Sample ID	Field (ug/L)	Lab (ug/L)	Pixel Value	Sample ID	Field (ug/L)	Lab (ug/L)	Pixel Value
1	5.3	3.21	29.0	24	5.7	12.04	33.0
2	5.2	2.37	28.0	25	6.6	5.96	37.0
3	3.9	2.93	30.0	26	8.7	18.04	38.0
4	4.2	1.22	30.0	27	6	9.08	40.0
5	4.5	2.89	31.0	28	7.3	10.91	40.0
6	4.8	2.05	31.0	29	5.5	3.24	40.0
7	5.5	2.66	29.0	30	7.7	11.48	35.0
8	5	3.9	30.0	31	9.8	10.86	43.0
9	4.4	3.18	28.0	32	9.3	9.66	42.0
10	5.2	3.51	27.0	33	12.7	12.07	40.0
11	5.1	4.86	28.0	34	8.8	9.26	53.0
12	5.4	8.21	31.0	35	8.2	10.06	45.0
13	5.9	7.37	35.0	36	9.6	14.23	40.0
14	6.4	4.9	37.0	37	16.08	19.71	38.0
15	5.8	15.41	42.0	38	17.06	17.52	39.0
16	10.6	6.79	43.0	39	10.6	9.77	37.0
17	8.1	8.47	40.0	40	11.4	6.25	34.0
18	6.4	12.98	37.0	41	13.9	7.48	38.0
19	6.1	11	31.0	42	10.6	10.88	41.0
20	8.3	9.46	40.0	43	12.7	11.32	41.0
21	3.9	4.84	31.0	44	18.7	35.45	45.0
22	5	4.17	37.0	45	7.5	10.49	40.0
23	6.3	8.69	37.0				

Table 6– Field Measurement Data and Lab Analysis Data from Each Sampling Site, and the Imagery Pixel Value of Spatial Corresponding Location. (Imagery processed by Algorithm 3)

Sample ID	Field (ug/L)	Lab (ug/L)	Pixel Value	Sample ID	Field (ug/L)	Lab (ug/L)	Pixel Value
1	5.3	3.21	0.277	24	5.7	12.04	0.312
2	5.2	2.37	0.273	25	6.6	5.96	0.287
3	3.9	2.93	0.289	26	8.7	18.04	0.314
4	4.2	1.22	0.272	27	6	9.08	0.302
5	4.5	2.89	0.289	28	7.3	10.91	0.318
6	4.8	2.05	0.277	29	5.5	3.24	0.270
7	5.5	2.66	0.289	30	7.7	11.48	0.318
8	5	3.9	0.278	31	9.8	10.86	0.331
9	4.4	3.18	0.263	32	9.3	9.66	0.334
10	5.2	3.51	0.276	33	12.7	12.07	0.355
11	5.1	4.86	0.273	34	8.8	9.26	0.334
12	5.4	8.21	0.302	35	8.2	10.06	0.341
13	5.9	7.37	0.318	36	9.6	14.23	0.359
14	6.4	4.9	0.324	37	16.08	19.71	0.397
15	5.8	15.41	0.311	38	17.06	17.52	0.395
16	10.6	6.79	0.333	39	10.6	9.77	0.344
17	8.1	8.47	0.284	40	11.4	6.25	0.355
18	6.4	12.98	0.302	41	13.9	7.48	0.357
19	6.1	11	0.300	42	10.6	10.88	0.377
20	8.3	9.46	0.302	43	12.7	11.32	0.355
21	3.9	4.84	0.278	44	18.7	35.45	0.368
22	5	4.17	0.279	45	7.5	10.49	0.344
23	6.3	8.69	0.302				

Table 7-- Matrix of Correlation Coefficients (p-values based on 95% confidence level)		
	Field analysis data	**Lab analysis data**
Algorithm 1	0.57 p-value (8.5E-37)	0.56 p-value (4.3E-33)
Algorithm 2	-0.75 p-value (7.9E-18)	-0.73 p-value (3.8E-18)
Algorithm 3	0.88 p-value (1.8E-18)	0.68 p-value (1.5E-18)

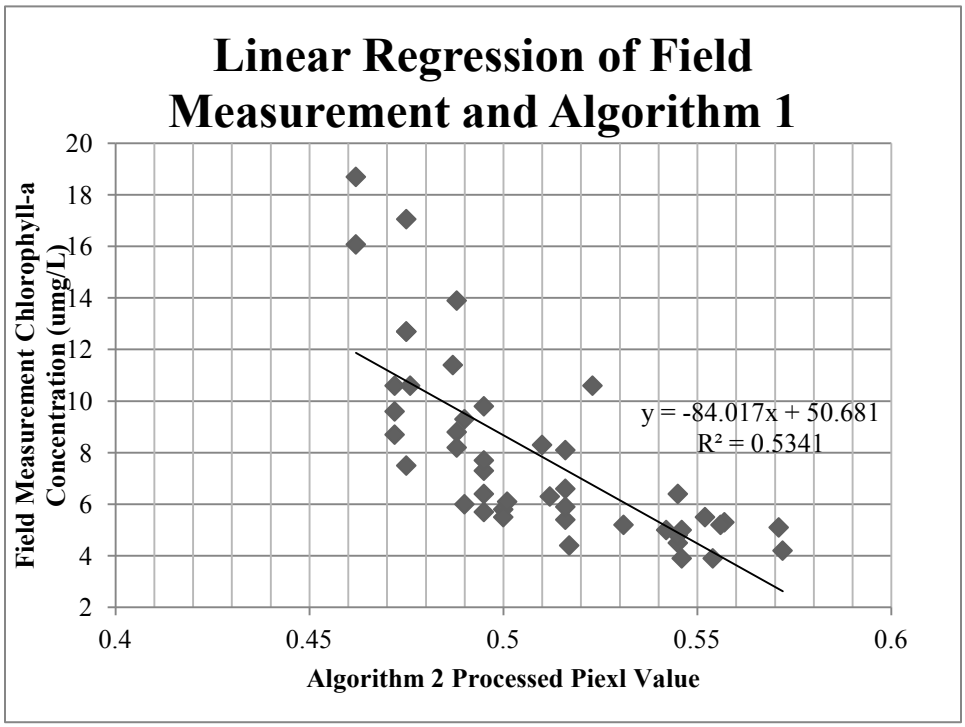

Figure 13-- Linear Regression of Field Measurement and Algorithm 1

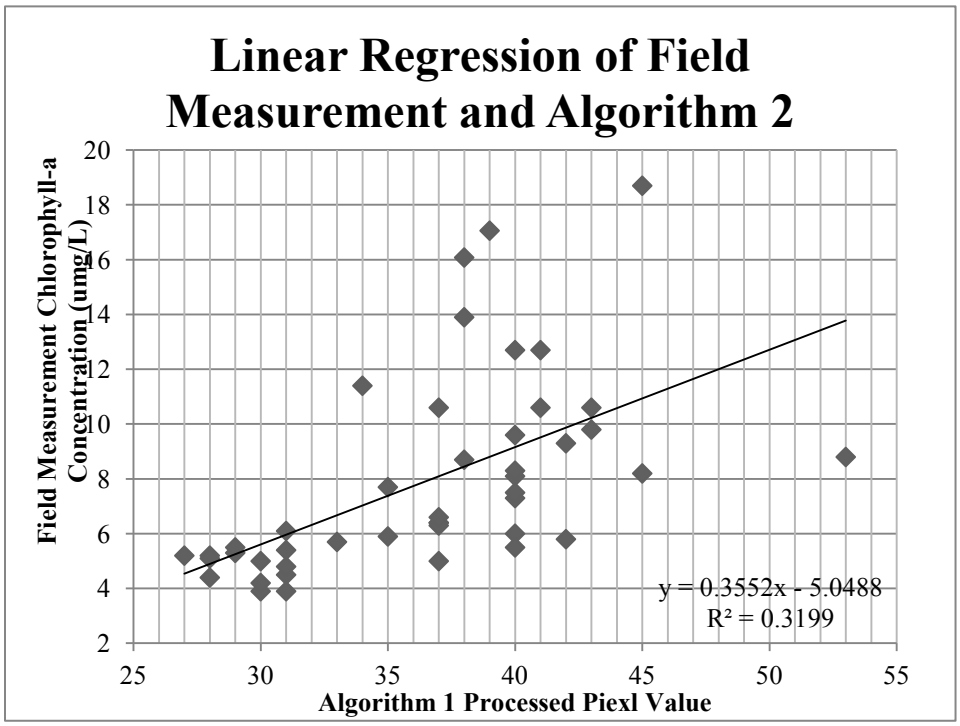

Figure 14-- Linear Regression of Field Measurement and Algorithm 2

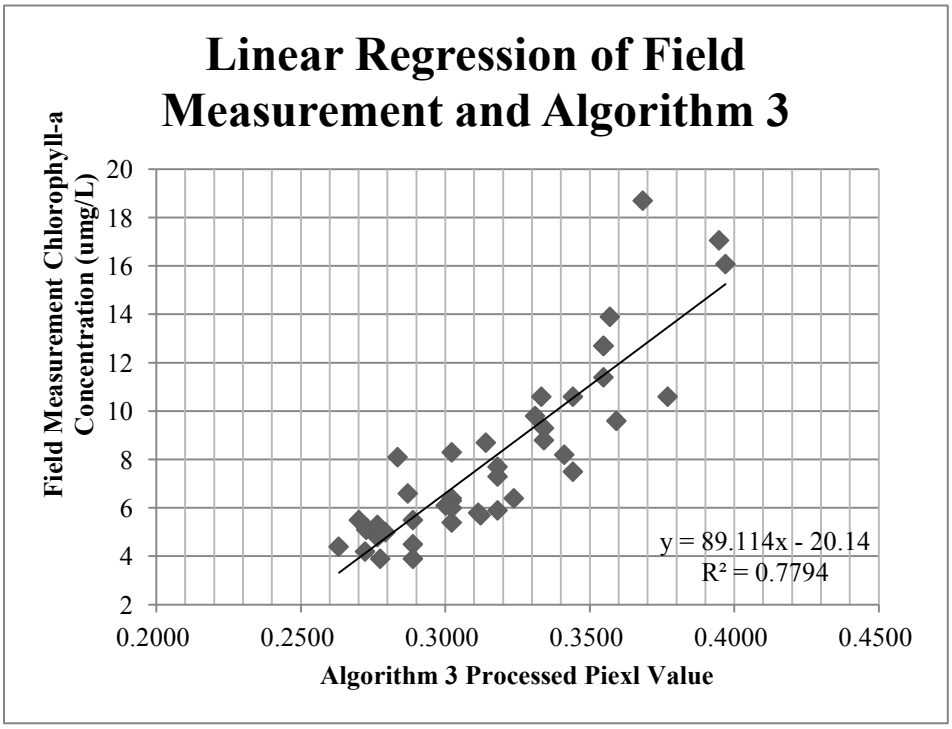

Figure 15-- Linear Regression of Field Measurement and Algorithm 3

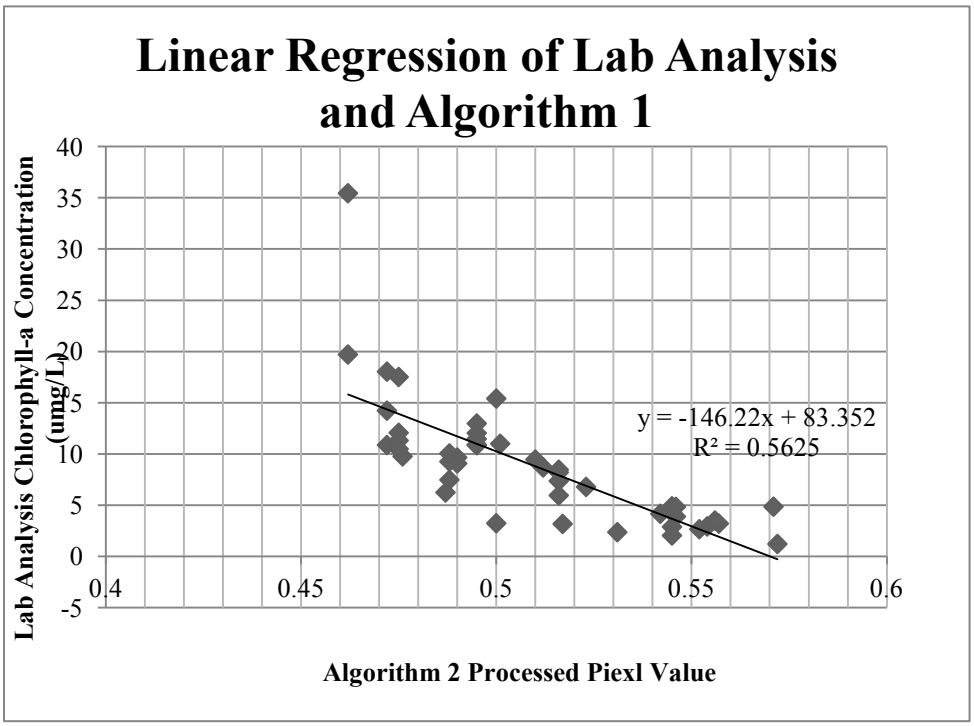

Figure 16-- Linear Regression of Lab Analysis and Algorithm 1

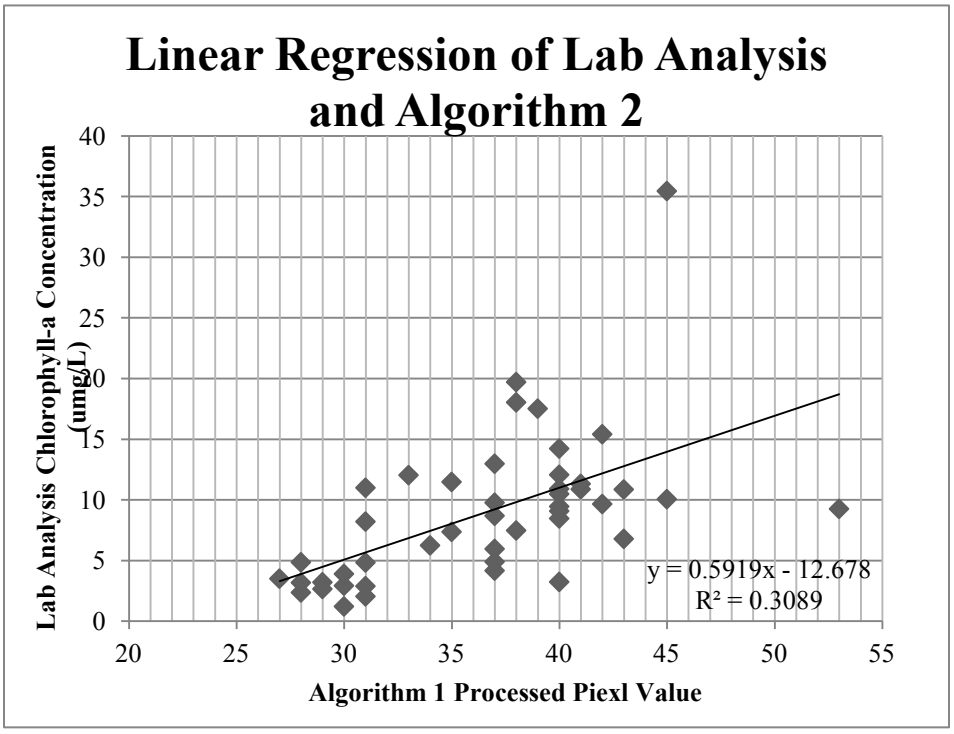

Figure 17-- Linear Regression of Lab Analysis and Algorithm 2

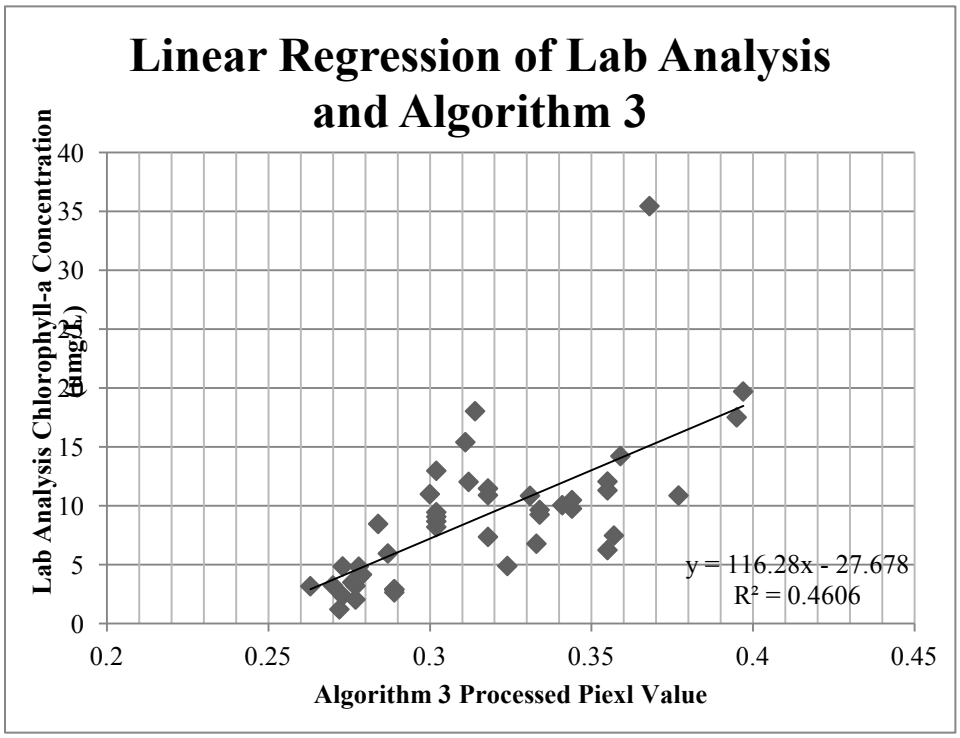

Figure 18-- Linear Regression of Lab Analysis and Algorithm 3

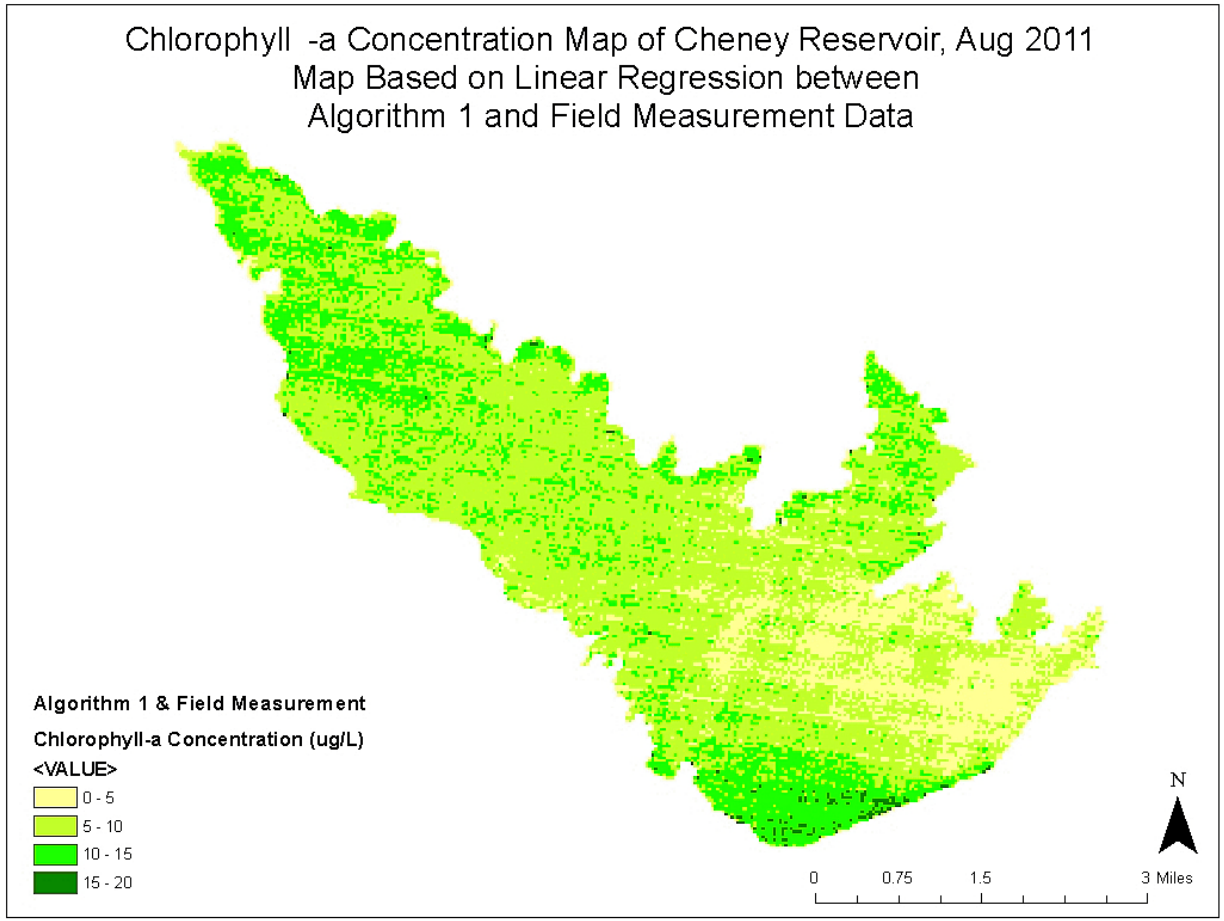

Figure 19 – Chlorophyll a Concentration Map of Cheney Reservoir, Aug 2011. (Algorithm 1 and Field Measurement)

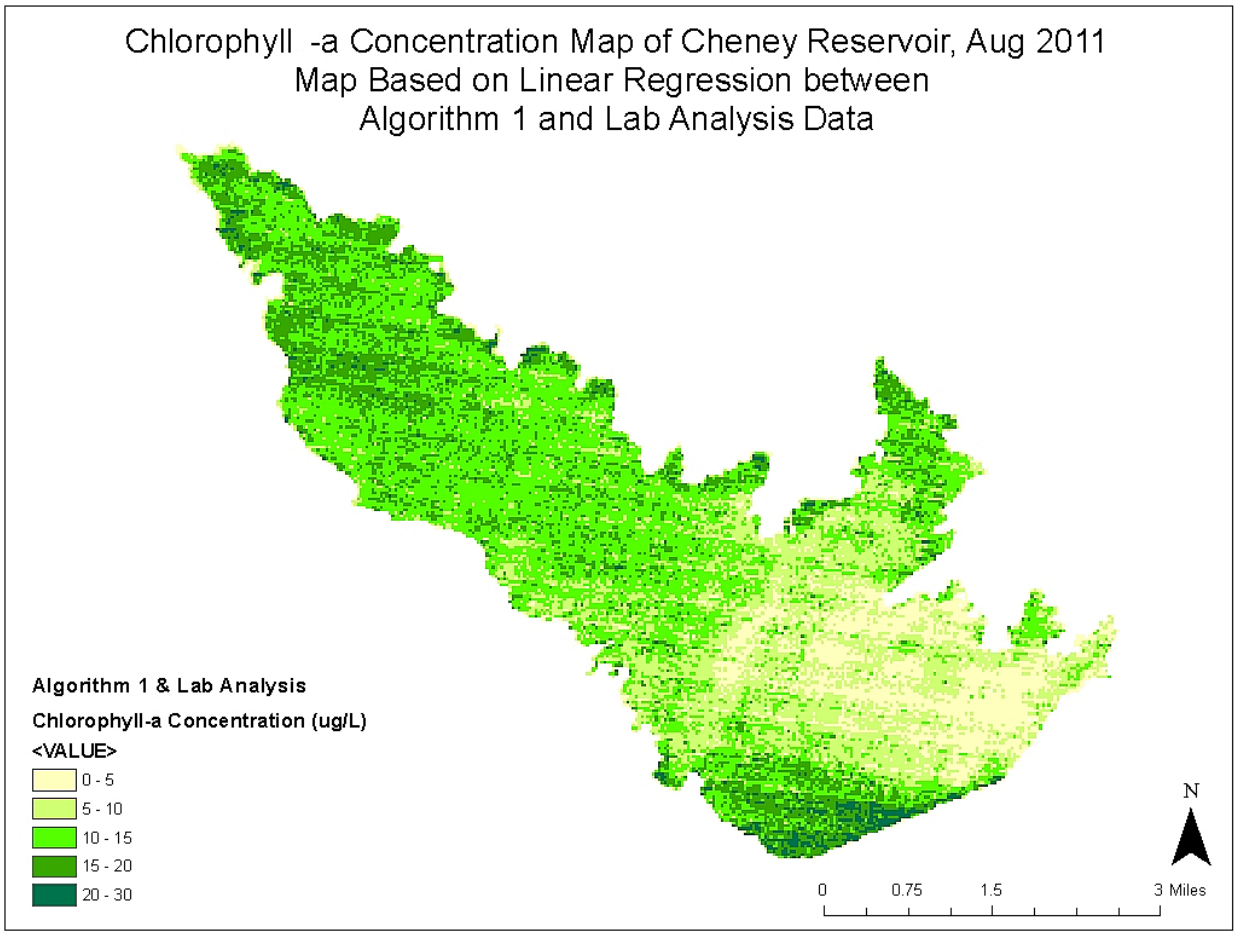

Figure 20 – Chlorophyll a Concentration Map of Cheney Reservoir, Aug 2011. (Algorithm 1 and Lab Analysis)

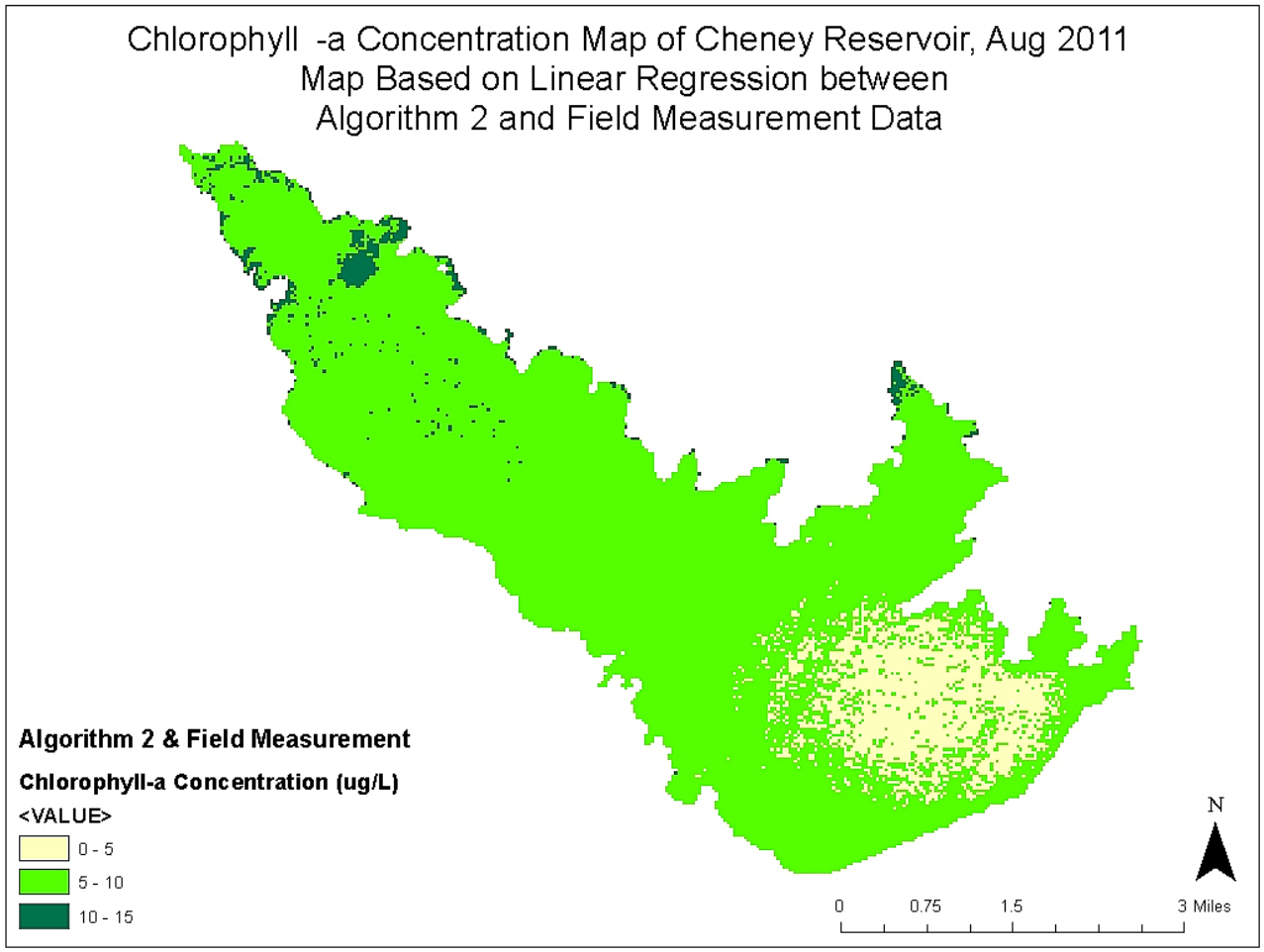

Figure 21 – Chlorophyll a Concentration Map of Cheney Reservoir, Aug 2011. (Algorithm 2 and Field Measurement)

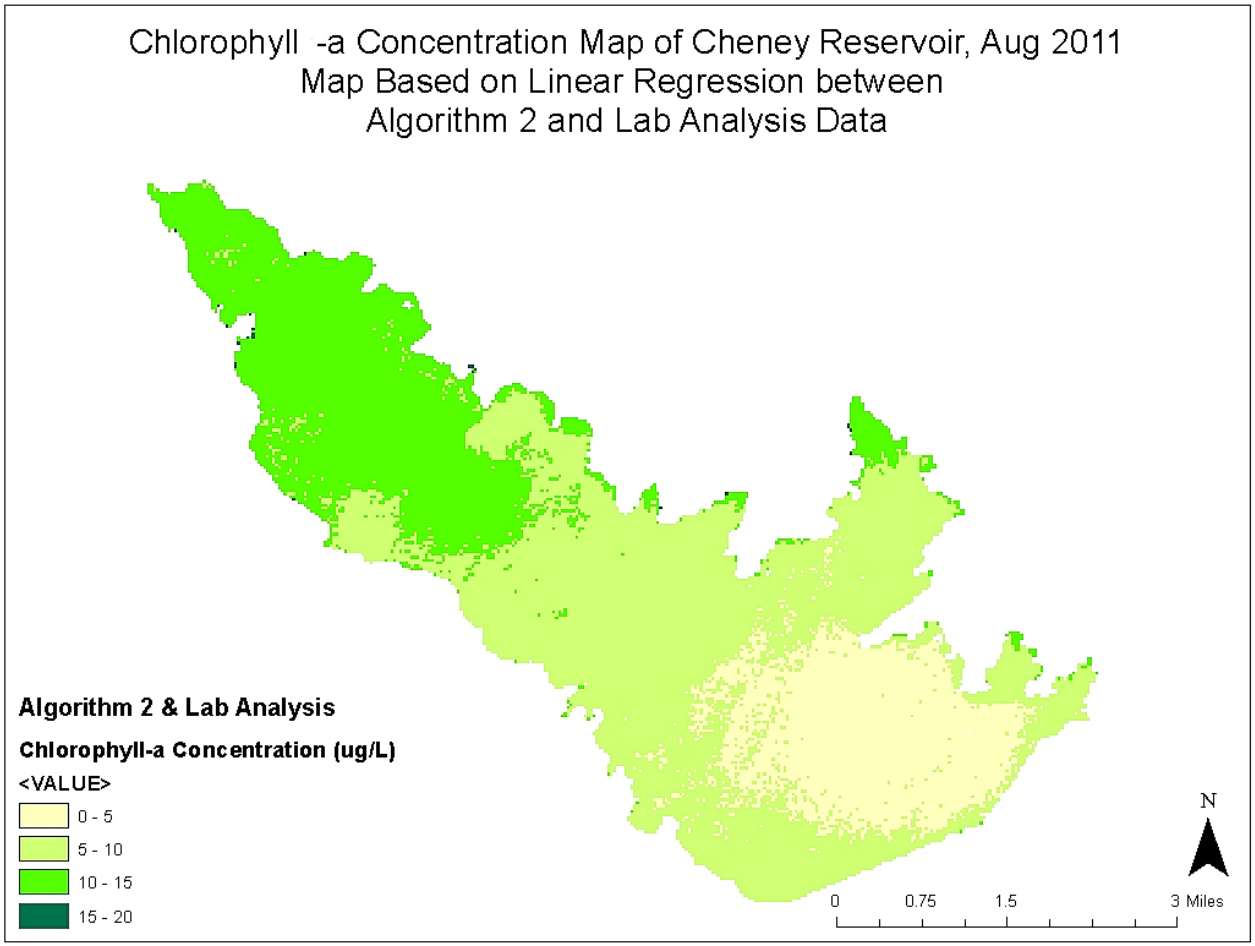

Figure 22 – Chlorophyll a Concentration Map of Cheney Reservoir, Aug 2011. (Algorithm 2 and Lab Analysis)

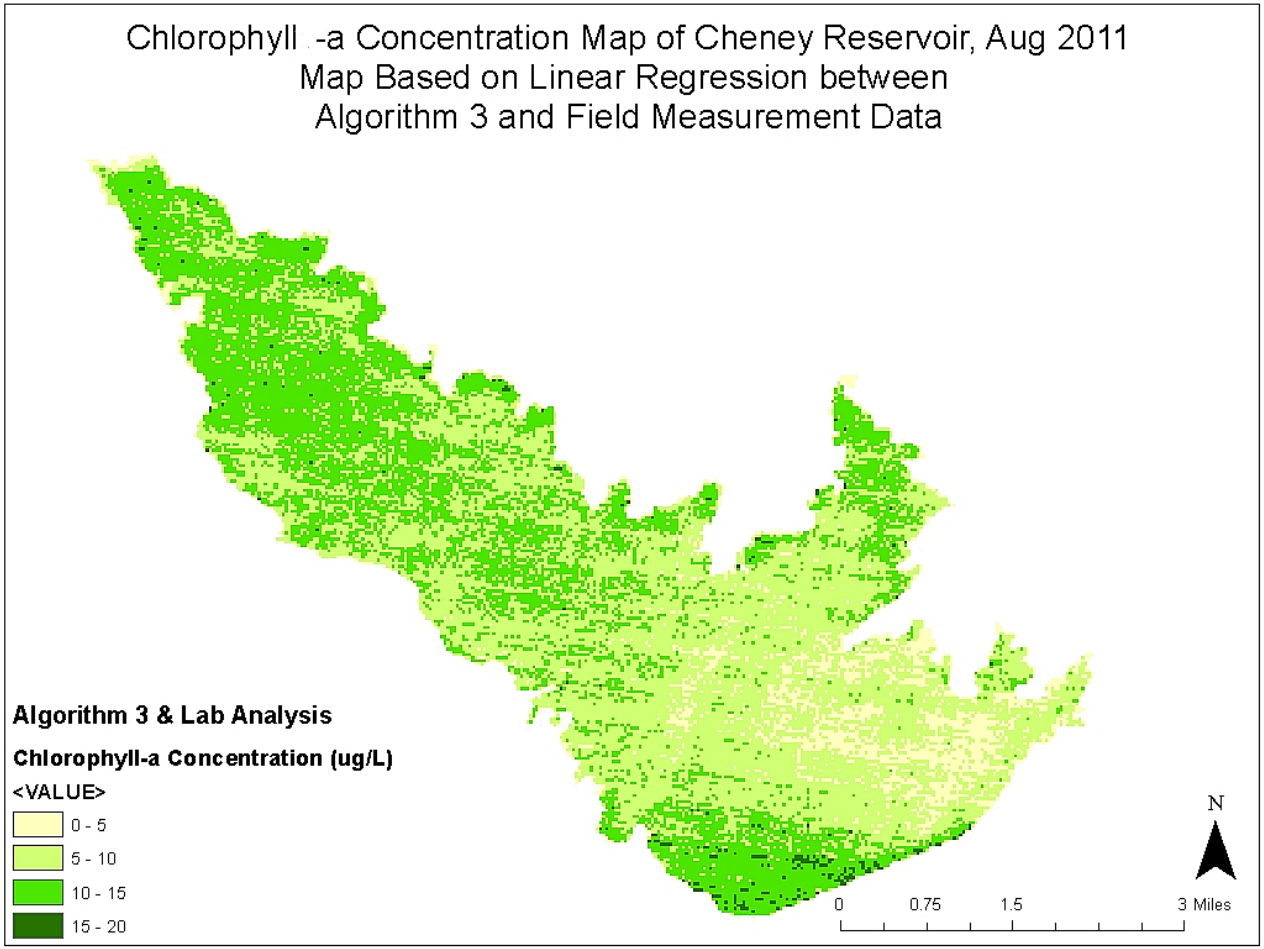

Figure 23 – Chlorophyll a Concentration Map of Cheney Reservoir, Aug 2011. (Algorithm 3 and Field Measurement)

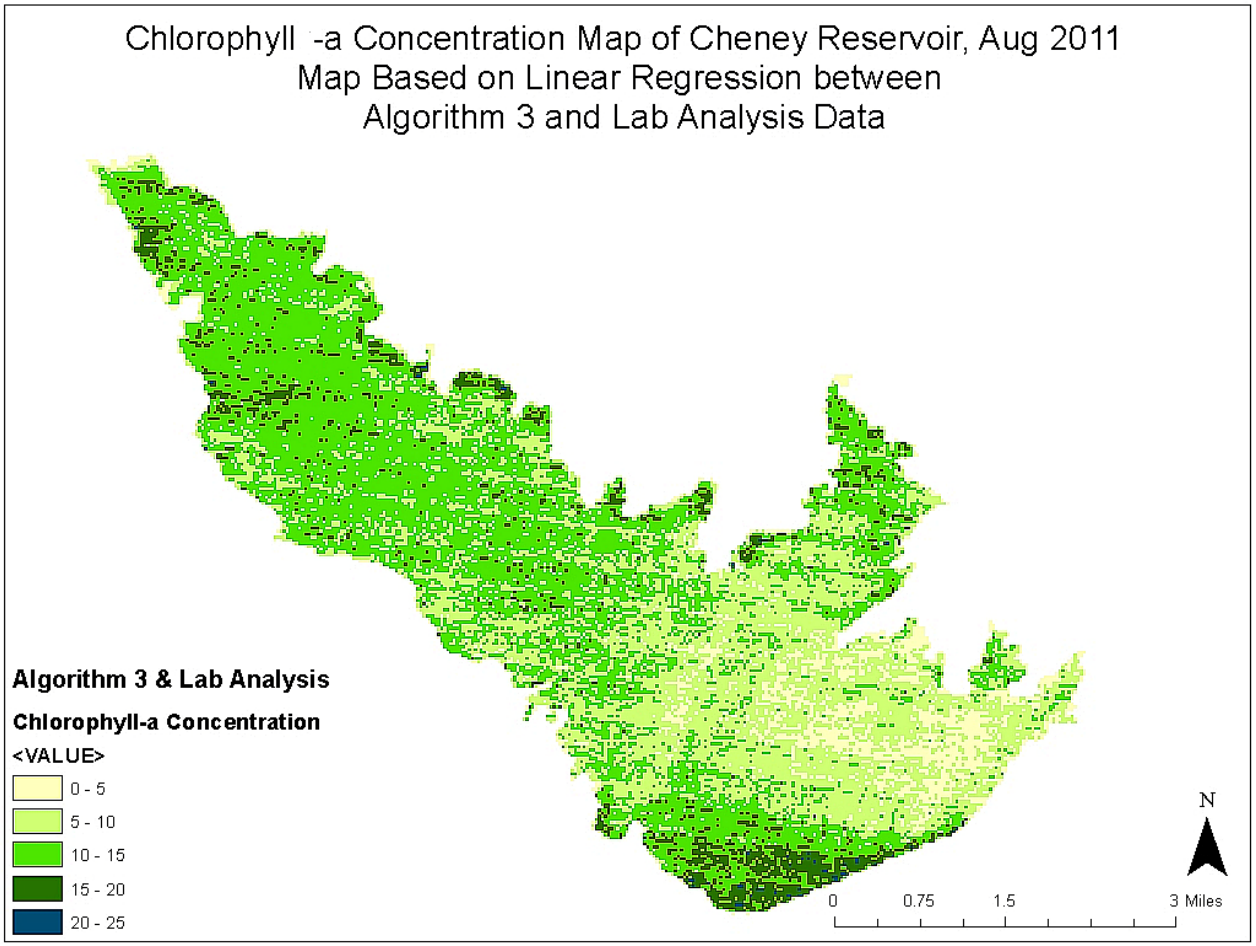

Figure 24 – Chlorophyll a Concentration Map of Cheney Reservoir, Aug 2011. (Algorithm 3 and Lab Analysis)

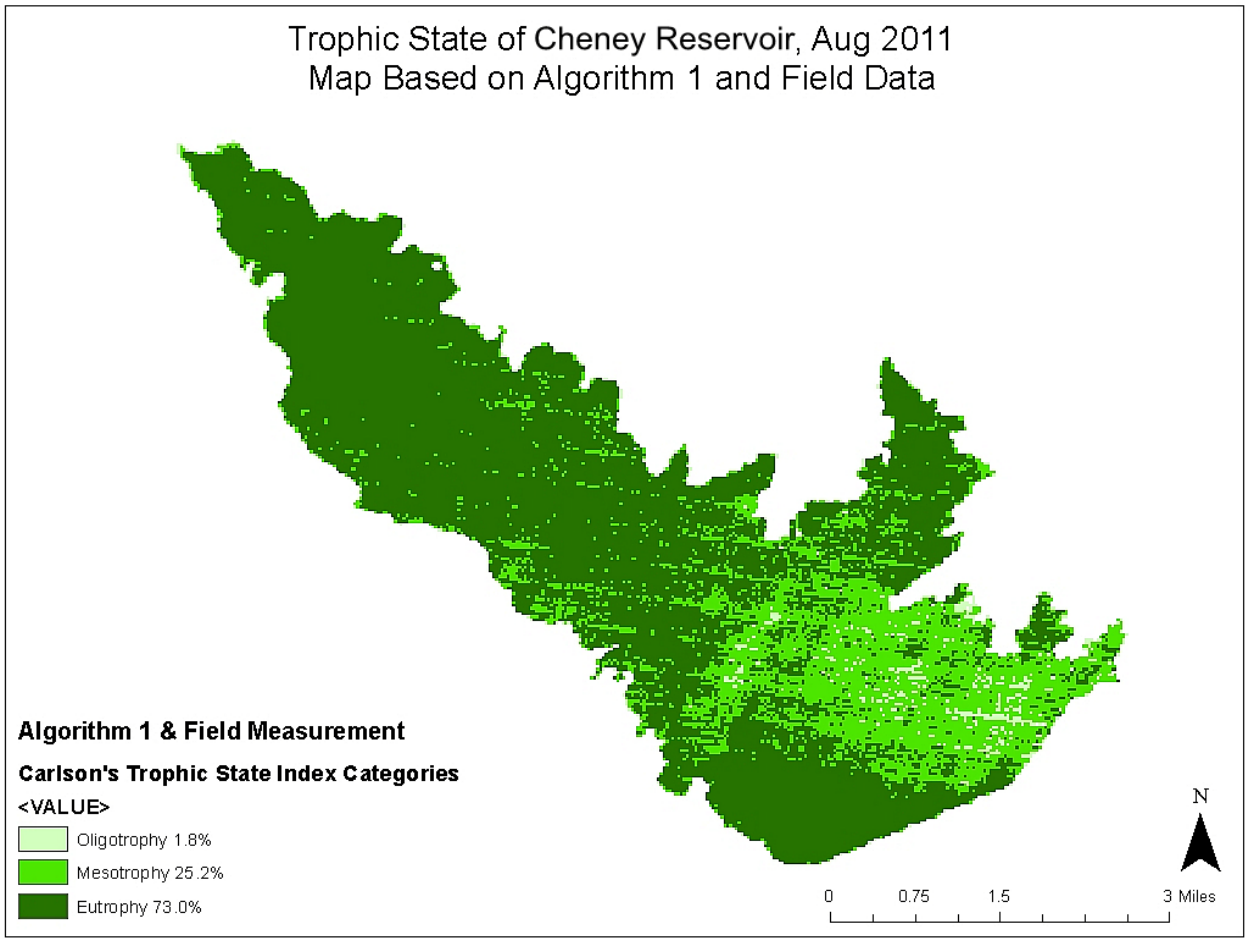

Figure 25 – Trophic State Map of Cheney Reservoir, Aug 2011. (Algorithm 1 and Field Measurement)

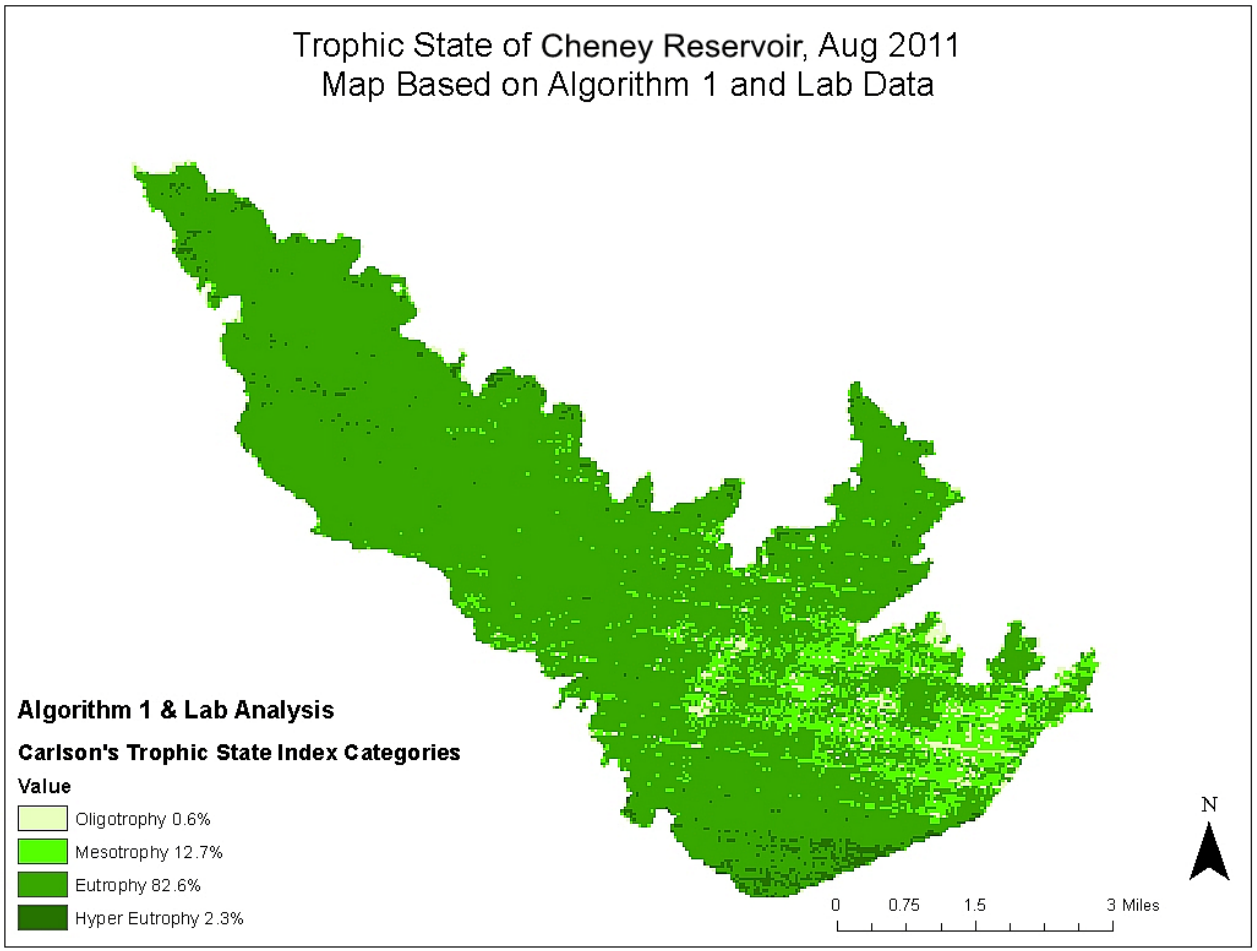

Figure 26 – Trophic State Map of Cheney Reservoir, Aug 2011. (Algorithm 1 and Lab Analysis)

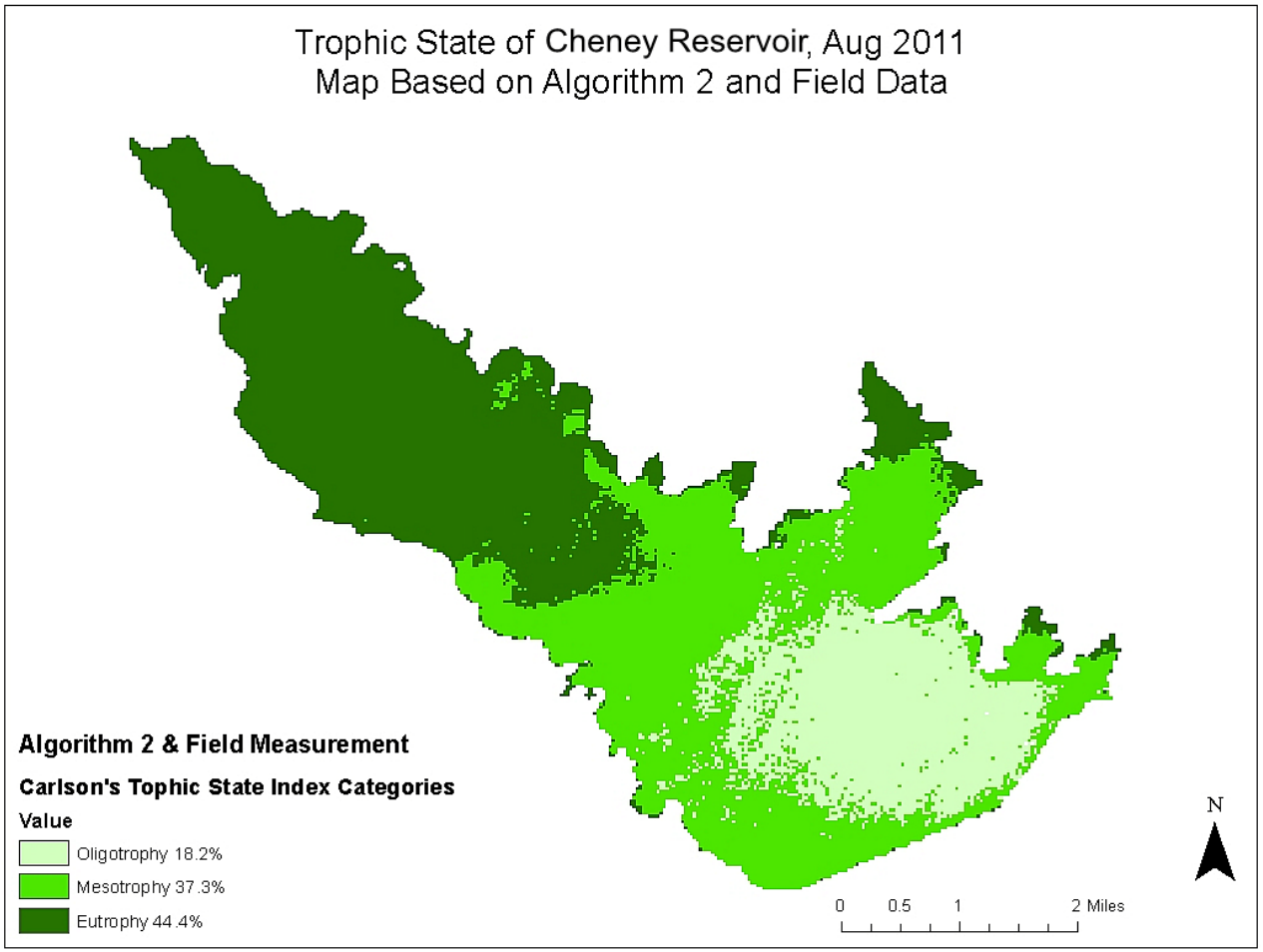

Figure 27 – Trophic State Map of Cheney Reservoir, Aug 2011. (Algorithm 2 and Field Measurement)

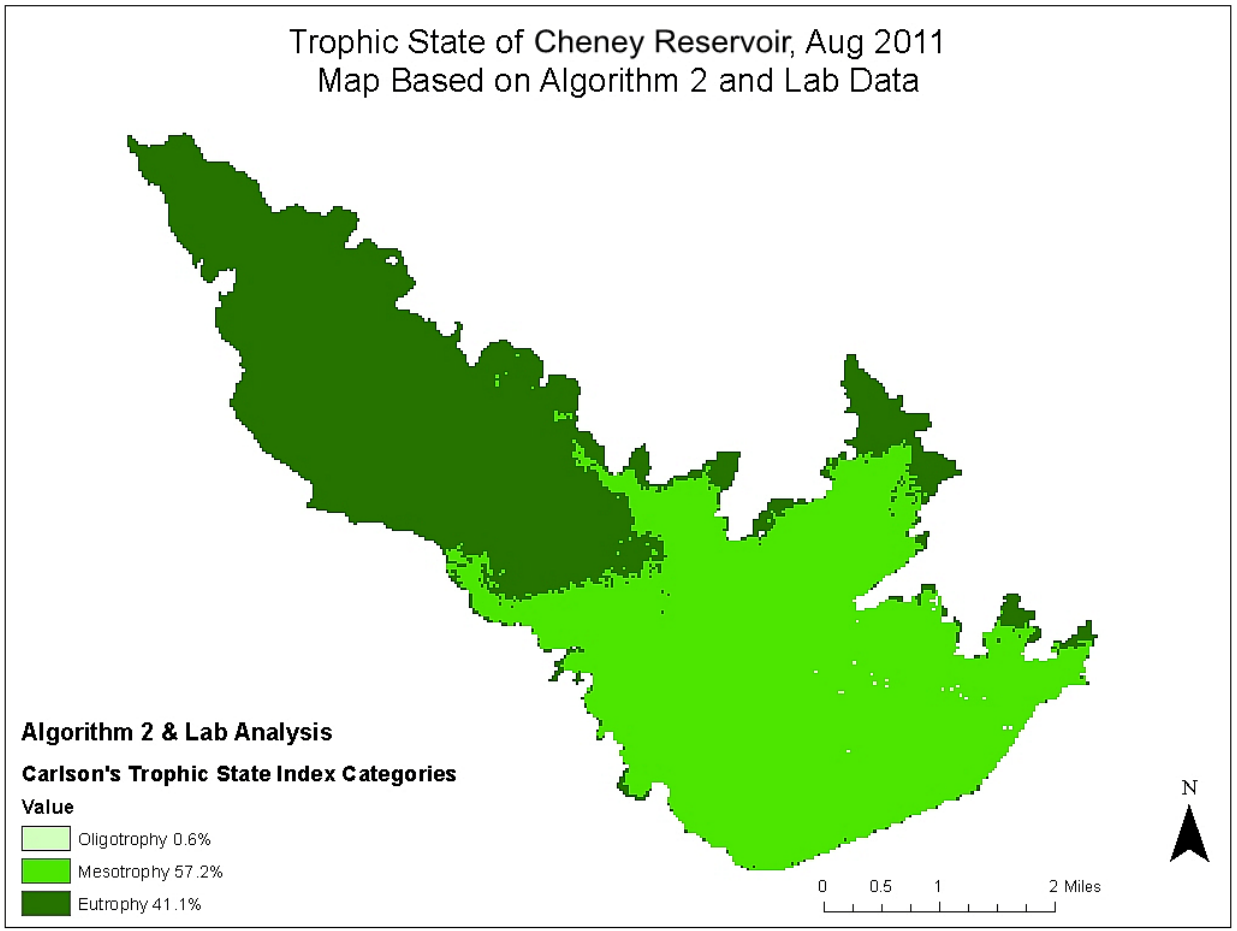

Figure 28 – Trophic State Map of Cheney Reservoir, Aug 2011. (Algorithm 2 and Lab Analysis)

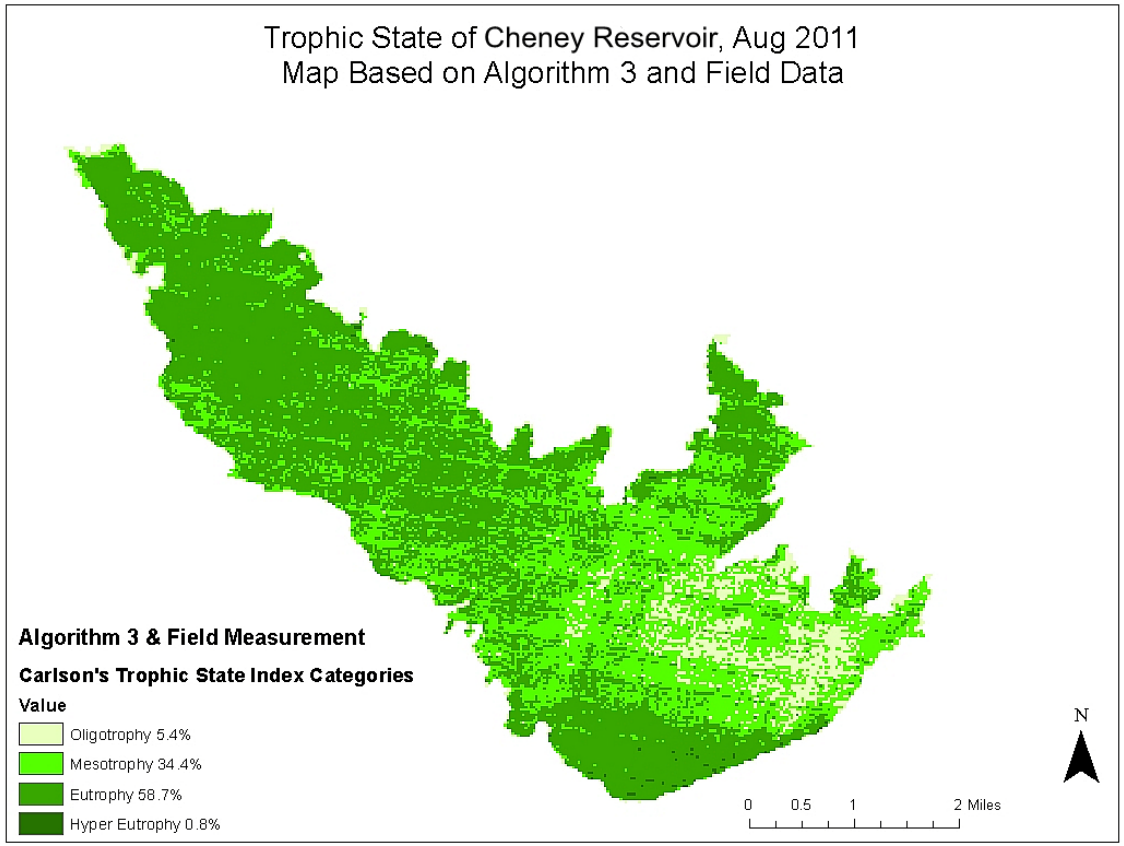

Figure 29 – Trophic State Map of Cheney Reservoir, Aug 2011. (Algorithm 3 and Field Measurement)

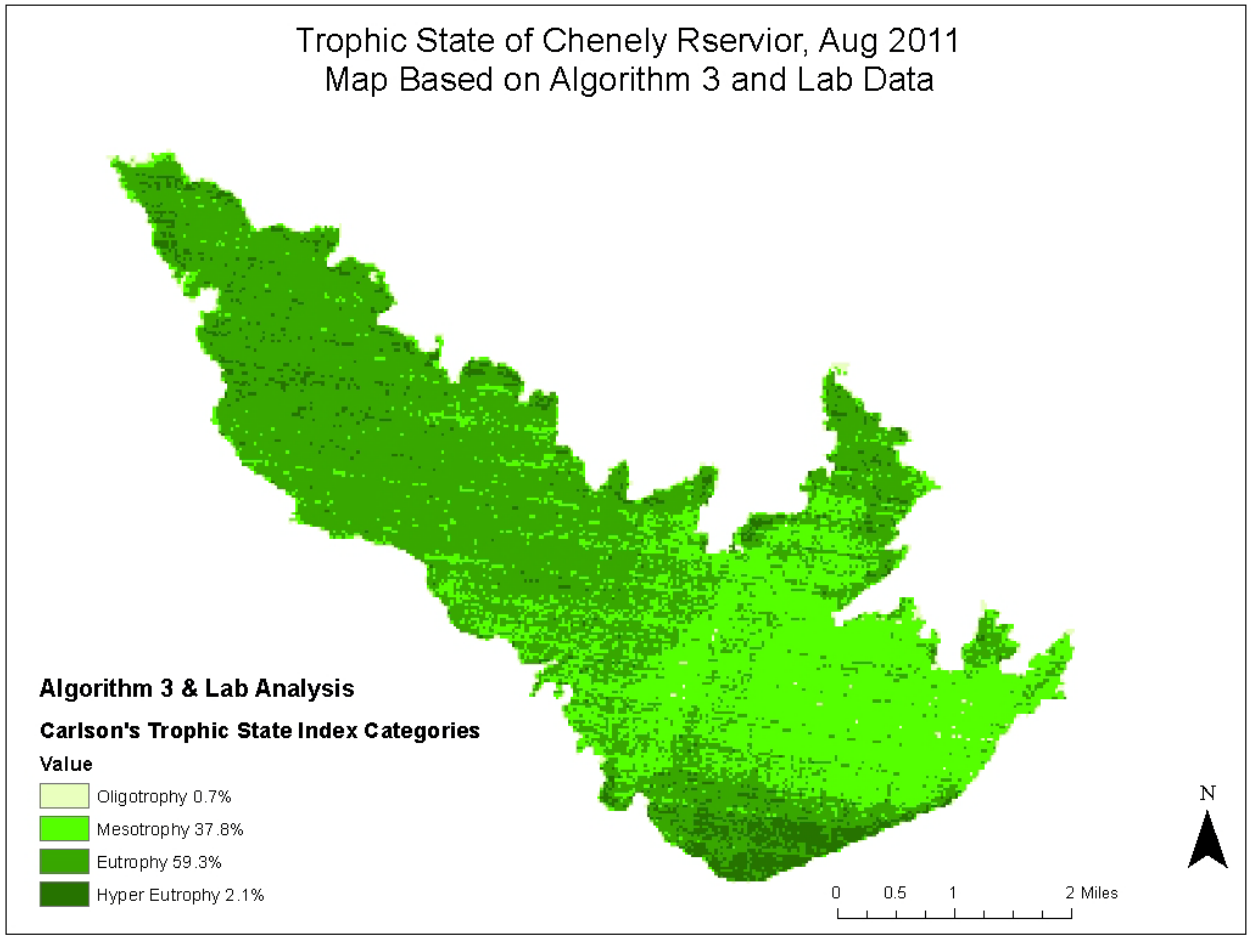

Figure 30 – Trophic State Map of Cheney Reservoir, Aug 2011. (Algorithm 3 and Lab Analysis)

4. Conclusion

Though there are many parameters, such as turbidity and temperature, associated with the Cheney Reservoir water which affect the reflectance characteristics of Landsat TM band 3 and band 4, those bands proved to be effective in isolating the reflectance feature associated with the concentration of chlorophyll a.

Most likely the major source of error for this analysis was the 14-days difference between the time of image acquisition (August 1, 2011) and the time when the chlorophyll-a measurements were taken (August 15, 2000). During this time, the algae in the reservoir may have easily been displaced by winds that mix the epilimnion (Smith, 2001). In order to track the changing of chlorophyll a concentration during these 14 days, data from a monitoring station is used for comparison. Figure 20 shows the fluctuation of total chlorophyll concentration from the monitoring station in August, 2011.

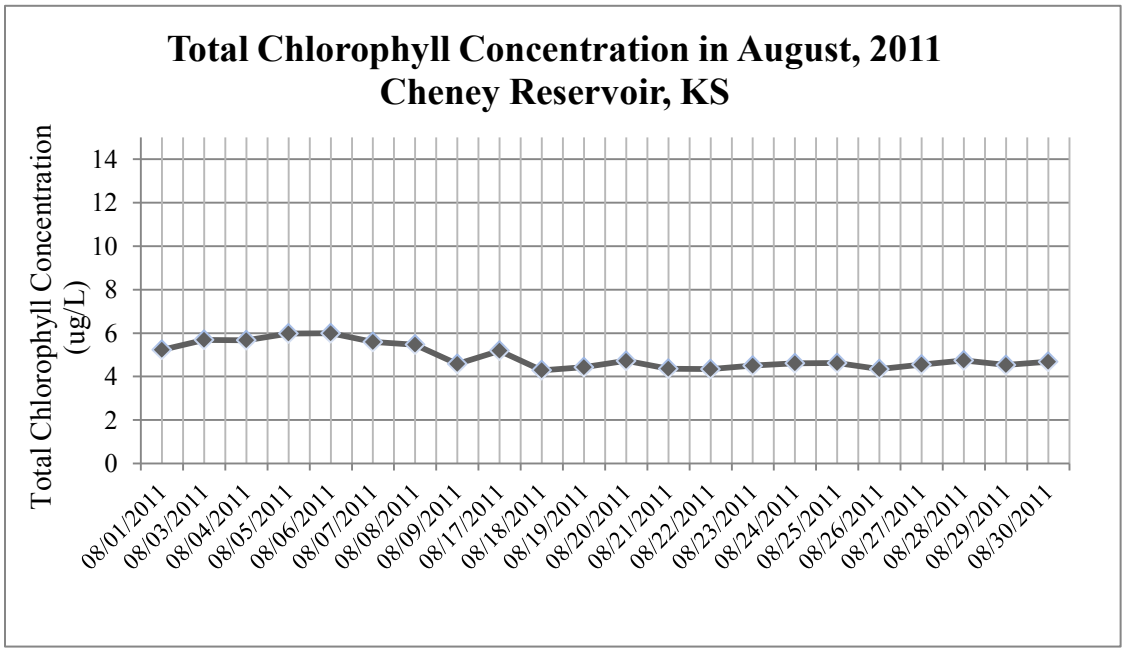

Figure 31 – Total Chlorophyll Concentration in August, 2011 in Cheney Reservoir, KS

Based on the data of the monitoring station, the coefficient of variation of 0.11 (standard deviation 0.56 ug/L associated with the mean value of 4.9 ug/L) seemed to be slight in the August 2011, compared with the 2011's annual coefficient of variation of 0.51 (annual stand deviation of 3.35 ug/L associated with the annual mean value of 6.56 ug/L). Slight coefficient of variation indicates a small changing of chlorophyll concentration during the 14 days, meaning the statistical relation was effecitve between the time of image acquisition (August 1, 2011) and the time when the chlorophyll-a measurements were taken (August 15, 2000).

Another problematic aspect emerges on the map products associated with algorithm 1 and 3, which show bright striping pattern noises. These bright stripes might be attributed to "bright-target recovery" (Barker, 1985). Figure 24 shows an image taken in 1996 offshore from Florida Key area that had a similar problem in this study's map results. In those problematic images, the detector's output values tend to be depressed after periods of saturation, such that scans away from bright targets could be significantly darker than the scans toward bright targets (Zhang, et al, 1999). This "bright-target recovery" theory can explain the bright striping noises only emerges on the map products associated with algorithm 1 and 3, however not on the map products associated with algorithm 2. Since algorithm 2 calculates the simple ratio between band 3 and band4, possibly reduced or eliminated the changes on the water-leaving radiance, which causes the bright stripes.

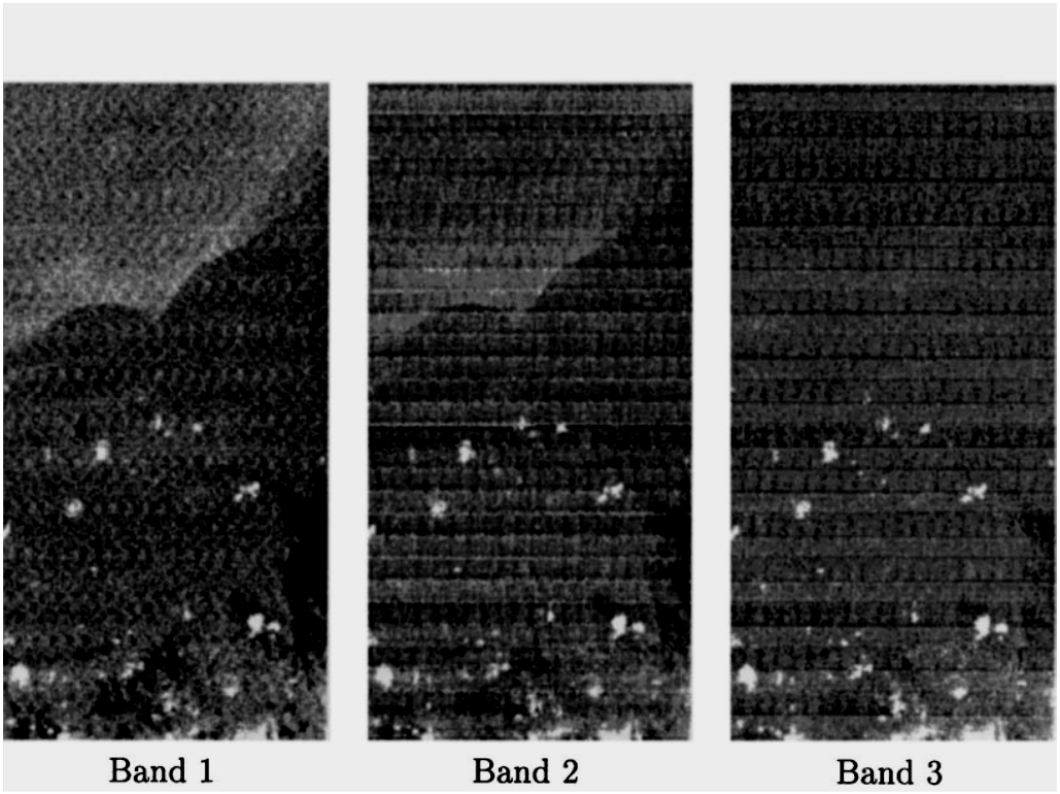

Figure 32- Images taken in 1989 and 1996 offshore from Florida Keys area November 5, 1996.

Interestingly, all maps of the chlorophyll a distribution and trophic state show a distinctive pattern with a low trophic area in the east of Cheney Reservoir and a eutrophic area in the west, which is the major inflowing area. The North Fork Ninnescah River is the major inflow to Cheney Reservoir and accounts for approximately 70% of the water flowing into the reservoir (Graham, 2010), thus the eutrophic problem in the west reservoir is possibly caused by chemical loading from The North Fork Ninnescah River.

For the future research goals which would include the following:

1. Redo the analysis with better data. The main sources of error were in the 14-days differences in the time of image acquisition (August 1, 2011) and the time when

the chlorophyll-a measurements were taken (August 15, 2011). An analysis on data which do not have this time difference would help improving the efficacy of the procedure.

2. Automate the process: If the above procedure were taken for further research, the next ideal step would be to automate the procedure to make it more efficient and practical to use. Once more monitoring stations are built in Cheney Reservoir and the process become time tested; the goal of real-time map production would be attained.

REFERENCE

Angelo, J. A. (2006). Encyclopedia of Space and Astronomy. (p. 430). New York: Facts on File.

Bartholomew, P. J. (2002). Mapping and modeling chlorophyll-a concentrations in the Lake Manassas Reservoir using Landsat Thematic Mapper satellite imagery. Manuscript submitted for publication, Civil Engineering, Virginia State University, Blacksburg, Virginia.

Bee, S. (2009). Seasonal and Annual Changes in Water Quality in the Ohio River Using Landsatbased measures of Turbidity and Chlorophyll-a (thesis).

Bledzki, L. (2009). Secchi disk. In N. Nagabhatla (Ed.), Encyclopedia of Earth Washington, D.C.: National Council for Science and the Environment.

Christensen, V. G., Graham, J. L., Milligan, C. R., Pope, L. M., & Ziegler, A. C. U.S. Department of the Interior, U.S. Geological Survey. (2006). Water quality and relation to taste-and-odor compounds in the north fork ninnescah river and cheney reservoir, south-central kansas, 1997-2003. Reston, Virginia: U.S. Geological Survery.

Christopherson, O. W. (2012). Geosystems, an introduction to physical geography. Prentice Hall.

“Waters, soils, or habitats that are high in nutrients; in aquatic systems, associated with wide swings in dissolved oxygen concentrations and frequent algal blooms.” Committee on Environment and Natural Resources, 2000

Curran, P. J., 1983, Estimating Green LAI from Multispectral Aerial Photography, Photogrammeric Engineering and Remote Sensing, 49:1709-1720

Jones, A. A. (1997). Global Hydrology, Processes, Resources and Environmental Management. (p. 242). Prentice Hall.

Jensen, J. R. (2000). Remote Sensing of the Environment – an Earth Resource Perspective (p. 13). Prentice Hall.

Graham, Jennifer. "Kansas Real-Time Water Quality". Government Website. US Geological Survey Real-Time Water Quality Data for the Nation, October 6, 2010.

Lawrence, E., Jackson, A.R.W., and Jackson, J.M., 1998, Eutrophication, in Longman Dictionary of Environmental Science: London, England, Addison Wesley Longman Limited, p. 144-145.

Longhurst, A. (1998). Ecological geography of the sea. (p. 46). San Diego: Academic Press.

Lopez, C.B., Jewett, E.B., Dortch, Q., Walton, B.T., Hudnell, H.K. 2008. Scientific Assessment of Freshwater Harmful Algal Blooms. Interagency Working Group on Harmful Algal Blooms, Hypoxia, and Human Health of the Joint Subcommittee on Ocean Science and Technology. Washington, DC.

Lukaski, H. C. (1987). Methods for the Assessment of Human Body Composition: Traditional and New. American Society for Clinical Nutrition, 46, 537-56.

McGrew, J. C., & Monroe, C. B. (1993). Correlation: association of interval/ratio variables. In An Introduction to Statistical Problem Solving in Geography (pp.

196-201). Long Grove, IL: Waveland Press, Inc.

Nath, R. K., & Deb, S. K. (n.d.). Water-body area extraction from high resolution satellite images-an introduction, review, and comparison. International Journal of Image Processing, 3(6), 353-372.

Schalles, J. F., Gitelson, A. A., Yacobi, Y. Z., & Kroenke, A. E. (1998). Estimation of chlorophyll a from time series measurements of high spectral resolution reflectance in an eutrophic lake. Journal of Phycology , 34(2), 383-390.

Smith, V. H. (2002). Managing taste and odor problems in a eutrophic drinking water reservoir. Lake and Reservoir Management, 18(4), 319-323.

Stauffer, J. (1999). Water crisis, finding the right solutions. (pp. 10-20). New York: Black Rose Books Ltd.

Walker, W.W., (1984) Statistical Bases for Mean Chlorophyll-a Criteria, in Lake and Reservoir Management - Practical Applications, Proc. 4th Annual Conference, North American Lake Management Society, McAfee, New Jersey, pp. 57-62.

Wang, Z., Hong, J., & Du, G. (2008). Use of satellite imagery to assess the trophic state of. Environmental Pollution, 155, 13-19.